



Available online at [www.sciencedirect.com](http://www.sciencedirect.com)



Advances in Space Research 43 (2009) 1372–1390

**ADVANCES IN  
SPACE  
RESEARCH**  
*(a COSPAR publication)*  
[www.elsevier.com/locate/asr](http://www.elsevier.com/locate/asr)

## Space debris: Assessing risk and responsibility

Andrew M. Bradley<sup>a</sup>, Lawrence M. Wein<sup>b,\*</sup>

<sup>a</sup> Institute for Computational and Mathematical Engineering, Stanford University, Stanford, CA 94305, USA

<sup>b</sup> Graduate School of Business, Stanford University, Stanford, CA 94305, USA

Received 12 August 2008; received in revised form 10 February 2009; accepted 11 February 2009

### Abstract

We model the orbital debris environment by a set of differential equations with parameter values that capture many of the complexities of existing three-dimensional simulation models. We compute the probability that a spacecraft gets destroyed in a collision during its operational lifetime, and then define the sustainable risk level as the maximum of this probability over all future time. Focusing on the 900- to 1000-km altitude region, which is the most congested portion of low Earth orbit, we find that – despite the initial rise in the level of fragments – the sustainable risk remains below  $10^{-3}$  if there is high ( $>98\%$ ) compliance to the existing 25-year postmission deorbiting guideline. We quantify the damage (via the number of future destroyed operational spacecraft) generated by past and future space activities. We estimate that the 2007 FengYun 1C antisatellite weapon test represents  $\approx 1\%$  of the legacy damage due to space objects having a characteristic size of  $\geq 10$  cm, and causes the same damage as failing to deorbit 2.6 spacecraft after their operational life. Although the political and economic issues are daunting, these damage estimates can be used to help determine one-time legacy fees and fees on future activities (including deorbit noncompliance), which can deter future debris generation, compensate operational spacecraft that are destroyed in future collisions, and partially fund research and development into space debris mitigation technologies. Our results need to be confirmed with a high-fidelity three-dimensional model before they can provide the basis for any major decisions made by the space community.

© 2009 COSPAR. Published by Elsevier Ltd. All rights reserved.

**Keywords:** Space debris; Low Earth orbit; Mitigation; Antisatellite weapon test

### 1. Introduction

Orbital debris generated by 50 years of space activities poses a risk for operational spacecraft, which can collide in a catastrophic manner with either another large object (e.g., an upper stage rocket body) or with a smaller fragment generated by a previous collision or by a previous explosion of a large object (Liou and Johnson, 2008). A high-fidelity three-dimensional simulation model of low Earth orbit (LEO, which is the region between 200 and 2000 km altitude) predicts that – even with no future launches – the growth rate of collisional debris would exceed the natural decay rate in  $\approx 50$  years (Liou and Johnson,

2008). Moreover, the analysis in (Liou and Johnson, 2008) did not account for the Chinese anti-satellite weapon (ASAT) test that destroyed the FengYun 1C spacecraft in January 2007, which created the largest manmade orbital debris cloud in history (Liou and Portman, 2007). NASA's safety guidelines recommend limiting the postmission lifetime of spacecraft or upper stages in LEO to 25 years (NASA Safety Standard 1740.14, 1995). Because this measure will not prevent a positive growth-rate of debris (Liou and Johnson, 2005), it has been suggested that the removal of large intact satellites from space is also necessary (Liou and Johnson, 2006). Although the impact of satellite removal has been assessed (Liou and Johnson, 2007), currently there are no technologies that are technically feasible and economically viable (Liou and Johnson, 2006).

Space debris represents a textbook example of environmental economics (Perman et al., 2003): space is a public

\* Corresponding author.

E-mail addresses: [ambrad@stanford.edu](mailto:ambrad@stanford.edu) (A.M. Bradley), [lwein@stanford.edu](mailto:lwein@stanford.edu) (L.M. Wein).

good (i.e., despite the 1976 Bogota Declaration, in which eight equatorial countries claimed sovereignty over the portion of geosynchronous Earth orbit lying above their territory (Soroos, 1982), there are no well-defined and enforceable property rights and no countries are excluded from launching satellites) and debris is a pollutant. More specifically, LEO is a renewable stock resource (much like air or water), in that debris eventually dissipates, albeit on an extremely slow time scale.

The two fundamental issues in environmental economics are to determine the target level of pollution and to decide how to achieve this target. Regarding the first issue, we use the concept of sustainability (loosely defined as the highest utility that can be maintained for all future time), which has gained some popularity in recent years as an alternative to economic efficiency (Perman et al., 2003, Chapter 4) particularly for studying resources that – like outer space – have no substitutes and are in the infancy of their exploitation. More specifically, we introduce the maximum (over all future time) lifetime risk to an operational spacecraft (i.e.,  $\max_{t \geq 0} r^o(t)$  in Eq. (14)) as a measure of sustainability.

Regarding the second fundamental issue, there are a number of different instruments used in environmental economics to achieve the target pollution level: technology controls, ceilings or taxes on emissions, subsidies for pollution reduction, tradeable emissions permits, and non-compliance fees. In practice, technology controls are often used because of the difficulty of measuring emissions, pollution levels, or costs, and indeed the 25-year postmission deorbit guideline and the end-of-life passivation of rocket bodies and spacecraft (NASA Safety Standard 1740.14, 1995) are forms of technology control.

In this paper, we develop an ordinary differential equation (ODE) model that is a mean field approximation, incorporating physical principles for collision rates (Alberty and Silbey, 1997), decay rates (Rossi et al., 1994), and orbital trajectories (King-Hele, 1964), as well as rocket body and spacecraft characteristics (Kessler, 2000) and the fragmentation models and empirical distributions developed in Johnson et al. (2001). The model elucidates the nature of the ( $\geq 10$  cm) debris dynamics over both the medium (centuries) and long (millennia) term, and allows us to assess sustainability. We also use the model to estimate the damage (in terms of the future operational spacecraft that are destroyed in collisions) associated with a present-day launch or ASAT explosion, as well as the damage due to existing space objects. These damages provide a basis for quantifying one-time country-specific legacy costs and setting fees for launches and ASAT tests, which can reduce the amount of debris generation, create a compensation fund for destroyed spacecraft, and partially fund the research and development necessary to remove large objects from space.

## 2. The model

We study the collisional interactions among satellites between the altitudes 900 and 1000 km, ignoring the effects

of collisions in lower or higher orbits; we refer to this (900, 1000) km region of space, which is the location of nearly 60% of all predicted catastrophic collisions in LEO over the next 200 years (Liou and Johnson, 2008), as the shell of interest (SOI). Our model tracks the number of rocket bodies and three types of spacecraft over time, and the effective number of four types of fragments. The effective number weights each fragment by the fraction of time its orbit is in the SOI and the probability that it is hazardous or benign (as explained below); spacecraft and rocket bodies, which together are referred to as intact, are assumed to have circular orbits, and hence spend all of their orbital time in the SOI. Because our model treats the SOI in isolation, we perform a sensitivity analysis in Section 3.2 that allows fragments created in other shells to enter the SOI.

Some intact in LEO have a deorbit capability to facilitate a 25-year postmission lifetime in LEO in accordance with NASA guidelines (NASA Safety Standard 1740.14, 1995): at the end of its operational lifetime, such an intact immediately maneuvers to either an orbit with a lower perigee (typically below 600 km) from which it decays naturally from LEO within 25 years, or to a disposal orbit above 2500 km altitude (intacts operating in the SOI will typically choose the former option). By deorbit, we shall mean that the intact leaves the SOI. Consequently, we differentiate the total number of spacecraft ( $S(t)$ ) into three types: those that have a deorbit capability ( $S_d(t)$ ), those that do not and are still operational ( $S_n^o(t)$ ), and those that do not have a deorbit capability and are no longer operational ( $S_n(t)$ ). (We use the same symbol for two purposes: e.g.,  $S_d(t)$  is the effective number of satellites of type  $S_d$  at time  $t$ .) Future spacecraft are launched into the SOI at annual rate  $\lambda_o$ , and we assume that some recent spacecraft and a fraction  $\theta_d$  of all future spacecraft have a postmission deorbit capability. These spacecraft deorbit at rate  $\mu_o$ , where  $\mu_o^{-1}$  is the average operational lifetime. The majority of existing spacecraft in LEO and a fraction  $1 - \theta_d$  of future spacecraft do not have a postmission deorbit capability, and change category, from  $S_n^o$  to  $S_n$ , at rate  $\mu_n$ , and then deorbit naturally at rate  $\mu_n$ . Similarly, some upper stage rocket bodies immediately deorbit the SOI and do not appear in our model, while other rocket bodies ( $R(t)$ ) linger at the separation altitude and deorbit naturally at rate  $\mu_R$ ; these latter rocket bodies are inserted into the SOI at the annual rate  $\lambda_R$ . Although deorbiting of spacecraft and rocket bodies may actually take several months, sensitivity analysis (details not shown) reveals that our assumption of instantaneous deorbiting has a negligible impact on all of our results.

We assume passivation techniques (e.g., venting rocket bodies of residual fuel and discharging spacecraft batteries) are in place to prevent future explosions, and so debris is generated in our model only via collisions between satellites. Catastrophic collisions result in the fragmentation of both objects, whereas noncatastrophic collisions result in the fragmentation of the less massive object. Essentially all intact–intact collisions are catastrophic. We consider

fragments having a characteristic length  $\geq 10$  cm, generally the lower limit of what sensors in the U.S. Space Surveillance Network can resolve (Johnson et al., 2001). We refer to fragments as hazardous or benign depending on whether or not they can produce catastrophic collisions with intact; although fragments can be hazardous or benign to each other as well, this distinction is far less important because many fewer fragments are generated in fragment–fragment collisions. Hence, the effective fragment number is indexed by two symbols and will be written  $F_\tau^\kappa$ , where  $\kappa \in \{h, b\}$  refers to being hazardous or benign to intact and  $\tau \in \{R, S\}$  refers to the source of a fragment – rocket body or spacecraft. A particular fragment is not simply hazardous or benign to an intact: the uncertainty in collision velocity causes the properties of the fragment to determine the probability with which it is hazardous or benign in a particular collision. A particular fragment from source  $\tau \in \{R, S\}$ , therefore, increases the effective number of  $F_\tau^h$  and  $F_\tau^b$  by quantities that sum to one. Fragments deorbit at constant rate  $\mu_{F_\tau^\kappa}$ .

Satellites of types  $\alpha$  and  $\gamma$  participate in collisions at rate  $\beta_{\alpha\gamma}\alpha(t)\gamma(t)$  at time  $t$ , where  $\alpha, \gamma \in \{S, R, F_\tau^\kappa\}$ ; hence,  $\beta_{\alpha\gamma}$  is the number of collisions between satellites of types  $\alpha$  and  $\gamma$  per unit time per satellite of type  $\alpha$  per satellite of type  $\gamma$ . Because a satellite's cross section (which dictates its likelihood of collision) and mass (which determines the number of new fragments if it is involved in a collision) have a joint probability distribution, we cannot estimate in isolation the number of fragments resulting from a collision between two types of satellites. Rather, we assume that fragments of type  $F_\tau^\kappa$  are generated from collisions between satellites of types  $\alpha$  and  $\gamma$  at rate  $\delta_{\alpha\gamma}^{\tau\kappa}\alpha(t)\gamma(t)$  at time  $t$ , for  $\alpha, \gamma \in \{S, R, F_\tau^\kappa\}$  (a factor  $\frac{1}{2}$  is necessary if  $\alpha = \gamma$ ). For example, a collision between a rocket body and a spacecraft produces all four types of fragments: hazardous and benign fragments from both a rocket body and a spacecraft.

The effective number of spacecraft, hazardous fragments, benign fragments, and total fragments at time  $t$  are given by, respectively,  $S(t) \equiv S_n^o(t) + S_n(t) + S_d(t)$ ,  $F^h(t) \equiv F_R^h(t) + F_S^h(t)$ ,  $F^b(t) \equiv F_R^b(t) + F_S^b(t)$ , and  $F^s(t) \equiv F^h(t) + F^b(t)$ . Let  $U \equiv \{S, R, F_\tau^\kappa, F_S^h, F_S^b, F_R^h, F_R^b\}$  be the set of satellite types,  $U^h \equiv \{S, R, F_S^h, F_R^h\}$  be the set of satellite types hazardous to intact,  $U^F \equiv \{F_S^h, F_S^b, F_R^h, F_R^b\}$  be the set of fragment types, and  $U^I \equiv \{S, R\}$  be the set of intact types. The model is given by

$$\dot{R}(t) = \lambda_R - \sum_{\alpha \in U^h} \beta_{R\alpha} R(t) \alpha(t) - \mu_R R(t), \quad (1)$$

$$\dot{S}_n^o(t) = (1 - \theta_d) \lambda_o - \sum_{\alpha \in U^h} \beta_{S\alpha} S_n^o(t) \alpha(t) - \mu_o S_n^o(t), \quad (2)$$

$$\dot{S}_n(t) = \mu_o S_n^o(t) - \sum_{\alpha \in U^h} \beta_{S\alpha} S_n(t) \alpha(t) - \mu_n S_n(t), \quad (3)$$

$$\dot{S}_d(t) = \theta_d \lambda_o - \sum_{\alpha \in U^h} \beta_{S\alpha} S_d(t) \alpha(t) - \mu_o S_d(t), \quad (4)$$

$$\dot{F}_\tau^\kappa(t) = \frac{1}{2} \sum_{\alpha \in U} \sum_{\gamma \in U} \delta_{\alpha\gamma}^{\tau\kappa} \alpha(t) \gamma(t) - \mu_{F_\tau^\kappa} F_\tau^\kappa(t), \quad (5)$$

for  $\tau \in U^I$ ,  $\kappa \in \{h, b\}$ .

A key shortcoming of the model relates to our handling of fragment–fragment collisions. We assume that a fragment generated in a fragment–fragment collision inherits the same properties as its ancestral intact (i.e., rocket body or spacecraft). Because a fragment generated by a fragment–fragment collision would be smaller than its parent fragments, we view Eq. (5) as upper bounding the effect of fragment–fragment collisions, and then as a lower bound consider a variant of Eq. (5) that simply disregards fragment–fragment collisions (i.e., sets  $\delta_{\alpha\gamma}^{\tau\kappa} = 0$  for  $\alpha, \gamma \in U^F$ ). We will usually be ignoring fragment–fragment collisions. Hence, we refer to the version of the model that incorporates fragment–fragment collisions (i.e., with  $\delta_{\alpha\gamma}^{\tau\kappa} > 0$  for  $\alpha, \gamma \in U^F$ ) as the fragment–fragment version of the model; otherwise, the reader should assume that we are ignoring fragment–fragment collisions (i.e., setting  $\delta_{\alpha\gamma}^{\tau\kappa} = 0$  for  $\alpha, \gamma \in U^F$ ). The intact–intact parameter values are the same in both versions of the model. When we ignore fragment–fragment collisions, the intact–benign fragment parameter values account only for the loss of a benign fragment, and the intact–hazardous fragment parameter values account only for the breakup of the intact and the loss of a hazardous fragment.

## 2.1. Equilibrium analysis

The main goal of this subsection is to understand the long-term, or equilibrium, behavior of system (1)–(5). Toward this end, we consider a simpler model that tracks only two types of satellites, intact ( $I(t)$ ) and hazardous fragments ( $F(t)$ ), and ignores fragment–fragment collisions:

$$\dot{I}(t) = -\beta_{II} I^2(t) - \beta_{IF} I(t) F(t) - \mu_I I(t) + \lambda_I, \quad (6)$$

$$\dot{F}(t) = \delta_{II} I^2(t) + \delta_{IF} I(t) F(t) - \mu_F F(t). \quad (7)$$

We define the parameters in Eqs. (6) and (7) in terms of those in Eqs. (1)–(5) via

$$\beta_{II} = \max \beta_{\alpha\gamma}, \quad (8)$$

$$\beta_{IF} = \max \beta_{\alpha\zeta}, \quad (9)$$

$$\mu_I = \min \{ \text{if } \lambda_R > 0, \mu_R; \text{ else } \infty \}, \quad (10)$$

$$\quad \text{if } \theta_d < 1, \mu_n; \text{ else } \infty \}, \mu_o \}, \quad (11)$$

$$\lambda_I = \lambda_R + \lambda_o, \quad (11)$$

$$\frac{\delta_{II}}{\beta_{II}} = \frac{\delta_{IF}}{\beta_{IF}} = \max \left\{ \max \frac{\delta_{\alpha\gamma}^{\tau\kappa}}{2\beta_{\alpha\gamma}}, \max \frac{\delta_{\alpha\zeta}^{\tau\kappa}}{\beta_{\alpha\zeta}} \right\}, \quad (12)$$

$$\mu_F = \min \mu_\zeta, \quad (13)$$

for  $\alpha, \gamma \in U^I$ ,  $\zeta, \eta \in U^F$ ,  $\tau \in \{R, S\}$ ,  $\kappa \in \{h, b\}$ .

In the remainder of this subsection, we state mathematical results that are rigorously derived in Section B of Bradley and Wein (2008), which is an earlier version of this paper.

First, if  $I(0) = I^s(0)$ , where  $I^s(t) = R(t) + S_n^o(t) + S_n(t) + S_d(t)$  is the total number of intact in Eqs. (1)–(5), and  $F(0) = F^s(0)$ , then  $F(t) \geq F^s(t)$  for  $t \geq 0$ ; i.e., the

number of hazardous fragments in Eqs. (6) and (7) provides an upper bound on the number of fragments in Eqs. (1)–(5).

Second, the number of hazardous fragments  $F(t)$  in Eqs. (6) and (7) remains bounded, and hence the total number of fragments  $F^s(t)$  in (1)–(5) also remains bounded; this is the main result of this subsection. We also derive explicit expressions for the equilibrium number of intact and the equilibrium number of fragments for Eqs. (6) and (7).

Third, if all space participants fully comply with deorbit procedures for rocket bodies and spacecraft (i.e.,  $\lambda_R = 0$  and  $\theta_d = 1$ ), Eqs. (1)–(7) are identical as  $t \rightarrow \infty$  with identical parameters (e.g.,  $\delta_{IF} = \delta_{SF}^{Sh}$ ), with the exception that the factor  $\frac{1}{2}$  is absorbed into the parameter  $\delta_H$ .

Fourth, if we include the fragment–fragment term  $\delta_{FF}F^2(t)$  in Eq. (7), then the upper bounding of  $F^s(t)$  in Eqs. (1)–(5) by  $F(t)$  in Eqs. (6) and (7) still holds. There are two possibilities as  $t \rightarrow \infty$ : the number of hazardous fragments grows without bound, or the model approaches an equilibrium that is nearly identical to that of the model without fragment–fragment collisions (i.e., in which  $\delta_{FF} = 0$ ) (this case occurs with our set of parameter values under full compliance).

## 2.2. Parameter estimation

Values for the parameters in Eqs. (1)–(5) are estimated in (and displayed in) the Appendix using Monte Carlo integration. Using the empirical probability distributions in Johnson et al. (2001), we assign each fragment a random characteristic length, area-to-mass ratio, and magnitude and direction of change in velocity after a collision; the first two random variables dictate a fragment’s area and mass, while the third combines with the first two to give the hazard probability. In addition, each fragment’s source’s altitude is uniformly distributed within the SOI, and the direction of its post-collision change in velocity is uniformly distributed on the surface of the sphere. The collision rate parameters ( $\beta_{xy}$ ), the debris generation parameters ( $\delta_{xy}^{rk}$ ), and the decay rates are computed by taking expectations over the three probability distributions from Johnson et al. (2001) and the two uniform distributions.

In the simulation, each fragment is weighted by the fraction of time it resides in the SOI, which is derived using the equations of orbital mechanics (e.g., King-Hele, 1964, Chapter 3). In addition, a fragment from source  $\tau \in \{R, S\}$  is split between hazardous ( $F_\tau^h$ ) and benign ( $F_\tau^b$ ) by calculating the probability that a collision between it and an intact would be catastrophic, which occurs if the kinetic energy of the projectile in Joules is 40 times greater than the mass of the target in grams (Johnson et al., 2001).

To estimate the collision rate parameters, we use the ideal gas model (Alberty and Silbey, 1997) to derive an analytical expression for  $\beta_{xy}$  in terms of the mean relative velocity of satellites in the SOI (Johnson et al., 2001), the volume of the SOI, and the mean collision cross sections

of the various satellite types (using data from Kessler (2000) for intact and the above probability distributions for fragments). We apply the ideal gas model to each portion of the SOI at a particular latitude, and use the full catalog of satellite element sets from Space Track (2008) to derive an empirical distribution of effective spatial density of satellites vs. latitude to capture the fact that the spatial density of satellites – and hence the collision rate – is higher near the poles.

To estimate the debris generation parameters, we use Eq. (4) in Johnson et al. (2001), which specifies the number of fragments from a collision having characteristic length of at least a certain size, in terms of the mass of the two objects involved in the collision, the collision velocity, and whether the collision was catastrophic.

We estimate the decay rates as reciprocals of residence times. We set  $\mu_o^{-1} = 3$  years to reflect the historical average of a 3-year mission lifetime and the 25-year decay rule recommended by NASA safety guidelines (NASA Safety Standard 1740.14, 1995, 2005). To estimate  $\mu_R$ ,  $\mu_n$ , and  $\mu_{F^k}$ , we use data in Table 4 of Rossi et al. (1994) to equate the residence time of a satellite to 110 years divided by the average area-to-mass ratio for the satellite type, which is quantified using the probability distributions in Johnson et al. (2001) for fragments and the values in Kaula (1983) for intact.

To estimate the launch rate of new spacecraft into the SOI, we analyze the full catalog of satellite element sets at the end of 2007 from Space Track (2008), identify the satellites that were spacecraft, and determine the effective number of spacecraft in the SOI. Inspecting the annual launch rates of these spacecraft into the SOI over the past decade, we set  $\lambda_o = 3/\text{year}$ . A similar analysis for rocket insertions leads to  $\lambda_R = 1/\text{year}$ ; because only a few rocket launchers remain that do not enable rocket body deorbiting, we assume  $\lambda_R = 1/\text{year}$  for 10 years and  $\lambda_R = 0$  thereafter. While the spacecraft deorbiting guidelines have been implemented, they have not been fully adopted by major space agencies (Liou and Johnson, 2007), and we set  $\theta_d = \frac{2}{3}$  and perform a sensitivity analysis on  $\theta_d$  later.

The full catalog of satellite element sets from Space Track (2008) are also used to determine the initial conditions for rocket bodies, spacecraft, and fragments:  $R(0) = 183.3$ ,  $S(0) = 207.2$ , and  $F^s(0) = 955.5$ . We set  $S_n^o(0) = \frac{(1-\theta_d)\lambda_o}{\mu_o} = 3$  and  $S_d(0) = \frac{\theta_d\lambda_o}{\mu_o} = 6$ , which are the equilibrium values if we ignore collisions in Eqs. (2) and (4), and  $S_n(0) = S(0) - S_n^o(0) - S_d(0)$ . To allocate  $F^s(0)$  among the four fragment types, we assume that – aside from the FengYun 1C fragments, which are known to originate from a spacecraft – 90% of the initial fragments are from rocket bodies (our results are insensitive to this assumption) and use the simulated proportion of fragments of type  $F_\tau^k$  generated by the breakup of an intact (Section F).

## 2.3. Comparison to Liou and Johnson (2008)

NASA researchers have recently developed a three-dimensional simulation of near-Earth orbital space that

tracks each satellite over time (Johnson et al., 2001; Liou and Johnson, 2005, 2008). Satellite breakups produce fragments whose properties are drawn from the distributions described in Johnson et al. (2001), though with some modifications as described in Liou and Johnson (2008). We compare the results of the fragment–fragment version of our model against those presented in Liou and Johnson (2008) for the SOI (Nicholas Johnson, private communication), which provide mean values for 150- to 200-year simulation runs. We set  $\lambda_o = \lambda_R = S_n^o(0) = S_d(0) = 0$  to coincide with the assumptions in Liou and Johnson (2008): no future launches, full compliance with rocket body deorbiting, and all initial spacecraft are nonoperational and have no deorbit capability. The initial conditions evident in Fig. 8 of Liou and Johnson (2008) are  $\approx 490$  “intacts + mission-related debris” and 520 fragments. It is not indicated what proportion of intact are rocket bodies. Because intact rocket bodies are larger and more spatially clustered (Section C.3) than intact spacecraft, we must take care in determining our initial conditions for the comparison with Liou and Johnson (2008). In our initial conditions for the comparison, we set the initial number of rocket bodies to 183.3 (Space Track, 2008), the initial number of spacecraft to  $490 - 183.3 = 306.7$ , and the initial number of fragments to 520, which are allo-

cated among the four categories using the methods described earlier.

Fragment growth in both models is nearly linear for the first 200 years (Fig. 1), and our model underestimates the number of fragments after 200 years relative to Liou and Johnson (2008) by 8.6% (2356 vs. 2579). Our model overestimates the number of destroyed intacts (11.02 vs. 8.21) and the number of intact-intact collisions (4.38 vs. 2.65), underestimates the fraction of intact-fragment collisions that are catastrophic (0.33 vs. 0.44), and overestimates the fraction of fragment–fragment collisions that are catastrophic (0.81 vs. 0.67) (Table 1). Possible reasons for these discrepancies are given in Section 4.

### 3. Results

#### 3.1. Base-case results

Numerical solutions to both versions of Eqs. (1)–(5) (Fig. 2) reveal that in both cases, the total number of fragments increases in a convex manner for  $\approx 1500$  years. In the absence of fragment–fragment collisions, the total number of fragments approaches its asymptotic value ( $F^s = 4.7 \times 10^5, F^h = 3.1 \times 10^5$ ), while in the presence of fragment–fragment collisions the number of fragments grows without bound, blowing up at time  $t \approx 1473$  (although in another set of simulations we found that the fragment level remains bounded if all spacecraft deorbit after their mission, i.e., if  $\theta_d = 1$ ). The two versions of the model are nearly indistinguishable for the first 500 years (e.g., at 200 years,  $F^h(200) = 1006$  and 1015 in the absence and presence of fragment–fragment collisions). Hereafter, we assume there are no fragment–fragment collisions.

The catastrophic intact-fragment collisions are the least frequent type of collision over the first several hundred years, but eventually become the most common type of collision (Fig. 3a and b). Our primary metric for measuring the hazard is the probability that a spacecraft launched at time  $t$  will be destroyed (via an intact–intact or catastrophic intact-fragment collision) while it is still operational, which is

$$r^o(t) = 1 - \left( 1 - \sum_{z \in U^h} \beta_{Sz} \alpha(z) \right)^{\mu_o^{-1}}. \quad (14)$$

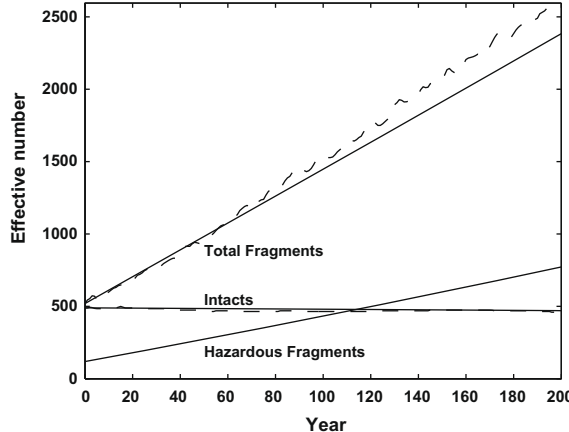


Fig. 1. Comparison of the fragment–fragment version of Eqs. (1)–(5) (—) to the results in Fig. 8 of Liou and Johnson (2008) (---). The model of Liou and Johnson (2008) does not distinguish between hazardous and benign fragments.

Table 1

Comparison of the fragment–fragment version of Eqs. (1)–(5) to Liou and Johnson (2008). For Liou and Johnson (2008), these are the average number of collisions (averaged over 150 Monte Carlo simulations) in the SOI for the results appearing in Fig. 8 in Liou and Johnson (2008) (Nicholas Johnson, private communication).

Object type	Number of collisions for the next 200 years		Catastrophic/non-catastrophic	
	(1)–(5)	Liou and Johnson (2008)	(1)–(5)	Liou and Johnson (2008)
Intact–intact	4.38	2.65	4.38/0.00	2.64/0.01
Intact–fragment	6.83	6.43	2.26/4.57	2.83/3.60
Fragment–fragment	0.58	0.58	0.47/0.11	0.39/0.19
Total	11.79	9.66	7.11/4.68	5.06/3.27

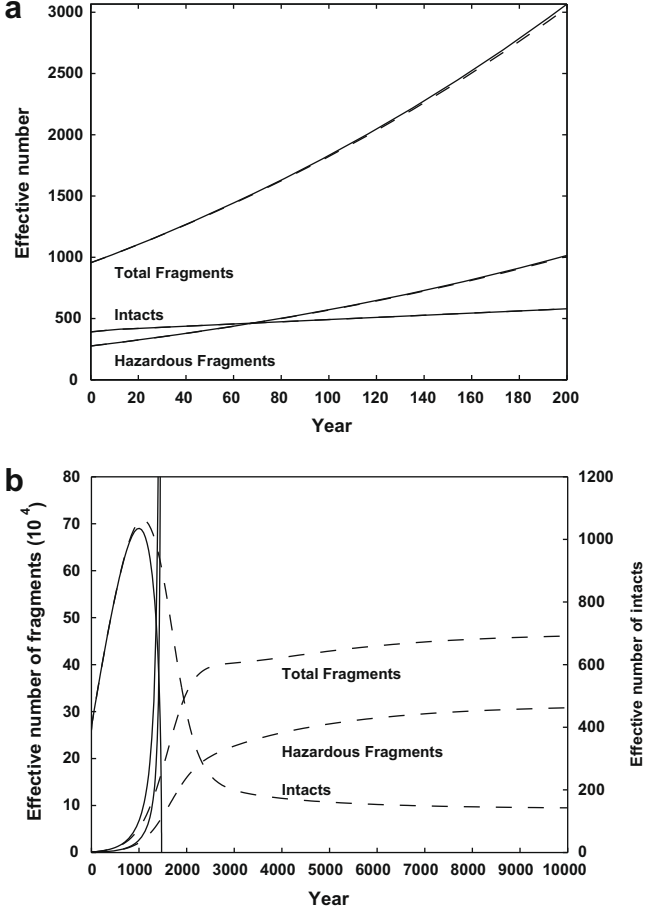


Fig. 2. The solution to both versions of Eqs. (1)–(5) for (a) 200 years and (b)  $10^4$  years. The dashed curves ignore fragment–fragment collisions, and the solid curves include fragment–fragment collisions.

Eq. (14) is constructed by considering the probability a particular operational spacecraft avoids a collision per year, raising the probability to a power equal to the mean operational lifetime, and subtracting the result from 1 to obtain the risk. This lifetime risk is initially  $1.84 \times 10^{-4}$  and increases to  $2.82 \times 10^{-4}$  in 200 years (Fig. 4a). However, this risk rapidly increases in  $\approx 1000$  years for  $\approx 2000$  years, eventually approaching the equilibrium value of  $2.19 \times 10^{-2}$  (Fig. 4b).

### 3.2. Sensitivity analyses

Because rocket bodies that do not immediately deorbit are only launched during the first 10 years in our model, our results are highly insensitive to the value of  $\lambda_R$ . We vary the spacecraft deorbit compliance rate  $\theta_d$  while keeping the other parameters fixed at their base-case value (Fig. 5). We define the sustainable lifetime risk to be the maximum of the lifetime risk over all future times, which is given by  $\max_{t \geq 0} r^o(t)$ , where  $r^o(t)$  is defined in Eq. (14). While the lifetime risk to an operational spacecraft over the next 200 years remains below  $4.2 \times 10^{-4}$  regardless of the value of  $\theta_d$ , the sustainable lifetime risk decreases to  $10^{-2}$  and

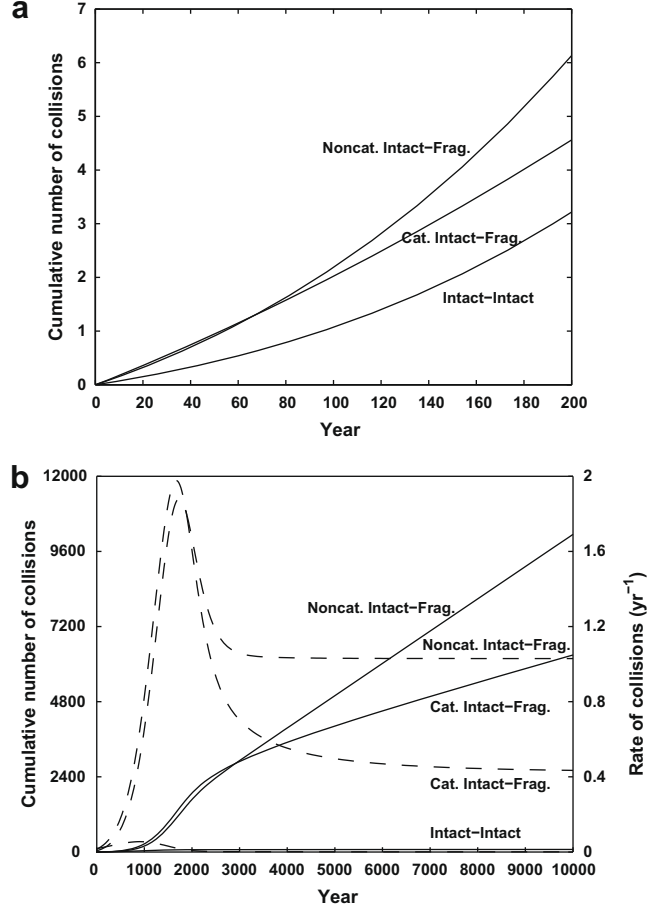


Fig. 3. (a) Cumulative number of intact–intact, catastrophic intact–fragment, and noncatastrophic intact–fragment collisions over the first 200 years and (b) cumulative number (—) and instantaneous rate (---) of these collisions over  $10^4$  years.

$10^{-3}$ , respectively, if the deorbit compliance increases to 84.9% and 98.2%, respectively. The sustainable lifetime risk drops sharply for very high compliance rates and is  $4.9 \times 10^{-4}$  under full compliance (i.e.,  $\theta_d = 1$ ).

In the full compliance case, the fragment level peaks at 10,800, which is 11.3-fold higher than the current level, after several millennia, and then approaches a very small equilibrium value ( $F^s = 2.61$ ). Under full compliance, if the spacecraft launch rate is increased 10-fold (e.g., due to the emergence of reusable launch vehicles), then the lifetime risk in 200 years is  $2.53 \times 10^{-4}$  and the sustainable lifetime risk is  $9.05 \times 10^{-4}$ .

Our model treats the SOI as isolated from all other altitudes. However, fragments often have eccentric orbits or decay from higher altitudes, and so fragments created outside the SOI can interact with satellites inside it. To understand the effect of this issue, we introduce a parameter  $\varepsilon$  into (5):

$$\dot{F}_\tau^\kappa(t) = \varepsilon \left( \frac{1}{2} \sum_{\alpha \in U} \sum_{\gamma \in U} \delta_{\alpha\gamma}^{\tau\kappa} \alpha(t) \gamma(t) \right) - \mu_{F_\tau^\kappa} F_\tau^\kappa(t). \quad (15)$$

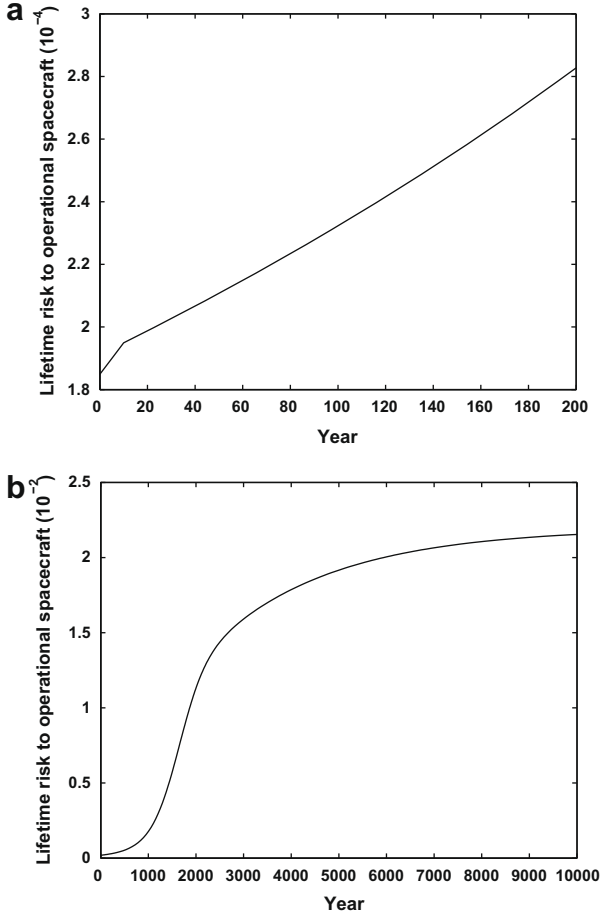


Fig. 4. The lifetime risk to an operational spacecraft (see Eq. (14)), which is the probability a spacecraft launched at a particular time will be destroyed (via an intact–intact or a catastrophic intact–fragment collision) while it is still operational, plotted vs. time for (a) 200 years and (b)  $10^4$  years.

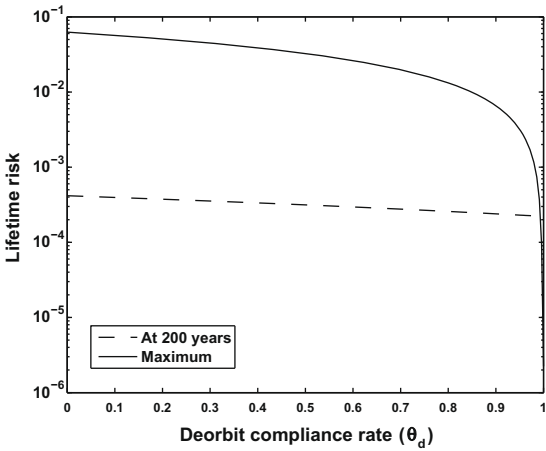


Fig. 5. The sustainable lifetime risk to an operational spacecraft, i.e.  $\max_{t \geq 0} r^o(t)$  in Eq. (14), (—) and the lifetime risk at  $t = 200$  years (---) vs. the proportion  $\theta_d$  of new launches that deorbit the spacecraft at the end of its operational life.

If  $\varepsilon > 1$ , then the number of fragments created in collisions is greater than in the nominal case  $\varepsilon = 1$ . The new fragments may be thought of as coming from a different shell

having dynamics similar to those of the SOI. We find that the sustainable lifetime risk and the lifetime risk after 200 years are approximately linear functions of  $\varepsilon$ . For  $\varepsilon = 2$ , the sustainable lifetime risk is 2.1 times greater, and the risk after 200 years is 1.2 times greater, than in the nominal case. Based on calculations similar to those in Section B.1,  $\varepsilon = 2$  is an overestimate of the value needed to account for fragments from other shells.

### 3.3. On the optimality of full deorbit compliance

Motivated by the results of the sensitivity analyses, we compute the optimal compliance rate from a societal, sustainable perspective. Let  $C_d$  be the cost to deorbit,  $C_S$  be the cost of a destroyed operational spacecraft,  $\theta_a$  be the attempted compliance rate,  $s$  be the probability that a deorbit attempt is successful (so that  $\theta_d = s\theta_a$ ), and  $r_{\max}^o(\theta_d)$  be the sustainable lifetime risk of an operational spacecraft (i.e.,  $r_{\max}^o(\theta_d) = \max_{t \geq 0} r^o(t)$ ) when the successful compliance rate is  $\theta_d$ . Then to minimize the sustainable costs related to spacecraft deorbiting and destruction, we solve  $\min_{\theta_a} \theta_a C_d + r_{\max}^o(s\theta_a) C_S$ .

We estimate the velocity requirements for deorbiting from the SOI to be  $\Delta v = 128$  m/s (Section B.1). Extrapolating from the cost estimates in Table 3 of Wiedemann et al. (2004) (which are in FY 2002 dollars), the additional launch cost  $\approx \$0.5M$  and the total development, production, and launch cost is about  $\$20M$ . We ignore the development and production cost, and assume the postmission deorbit cost is  $C_d = \$0.5M$ . The replacement cost of building and launching a new satellite is  $\approx \$0.2$ – $\$0.5B$  for a commercial, scientific, or weather satellite, or  $\approx \$0.5$ – $\$1.5B$  for a defense satellite (de Weck et al., 2003), and we set  $C_S = \$0.5B$ . The failure rate of propulsion systems has been estimated to be 3.9% (de Weck et al., 2003, Fig. 8) which yields  $s = 0.961$ . Substituting these values into the optimization problem and using the  $r_{\max}^o(\theta_d)$  function in Fig. 5, we find that  $\theta_a = 1$  is optimal.

To assess the robustness of this result, we determine how high the deorbit cost has to be to make  $\theta_a = 1$  no longer optimal, which occurs when either the derivative of the total sustainable cost with respect to  $\theta_a$  equals zero at  $\theta_a = 1$ , i.e.,  $C_d = -\frac{\partial r_{\max}^o(s\theta_a)}{\partial \theta_a} \Big|_{\theta_a=1} C_S$ , or when the cost at  $\theta_a = 0$  equals the cost at  $\theta_a = 1$ , i.e.,  $C_d = (r_{\max}^o(0) - r_{\max}^o(s))C_S$ . The breakeven value is  $C_d = \$30.0M$ , which is 60 times larger than the actual value and several million dollars more than the total cost estimate in Wiedemann et al. (2004). Although we omit the details, a similar derivation shows that 100% compliance of rocket body deorbiting is also optimal.

### 3.4. Assessing the damage due to space activities

A prerequisite for quantifying fees is to calculate the damage caused by various space activities. Toward this

end, we define the damage caused by a space activity to be the total number of destroyed operational spacecraft generated by this activity. If we let  $S^o(t) = S_n^o(t) + S_d(t)$  be the number of operational spacecraft at time  $t$ , then the number of destroyed operational spacecraft up to time  $T$  is

$$n_d(T) = \int_0^T S^o(t) \sum_{\gamma \in U^h} \beta_{S\gamma} \gamma(t) dt. \quad (16)$$

Let  $n_d^-(T)$  be the damage up to time  $T$  in the current environment, and  $n_d^+(T)$  be the damage up to time  $T$  after a perturbation has been applied at time 0. We define an activity's damage up to time  $T$  to be  $n_d^+(T) - n_d^-(T)$ . The perturbations are  $R(0) \rightarrow R(0) + 1$  for an extra rocket insertion,  $R(0) \rightarrow R(0) - 1$  and  $F_R^k(0) \rightarrow F_R^k(0) + \frac{\hat{N}(1600)s_R^{Rk}}{2}$  for a rocket breakup, and  $S_n(0) \rightarrow S_n(0) - 1$  and  $F_S^k(0) \rightarrow F_S^k(0) + \frac{\hat{N}(1600)s_S^{Sk}}{2}$  for a satellite breakup, where the latter two perturbations follow from Eq. (D.11) and  $\hat{N}(\cdot)$  and  $s_x^{tk}$  are defined in Eqs. (D.3), (D.4), and (D.7). For a new extra launch, we do not want to consider the self-inflicted damage if the newly-launched spacecraft is destroyed while it is operational, although we do want to capture the subsequent damage caused by the fragments of such a collision. Hence, for a new extra launch of a spacecraft with deorbit capability, we add the equation  $\dot{S}_d^u(t) = -\sum_{x \in U^h} \beta_{Sx} S_d^u(t) \alpha(t) - \mu_o S_d^u(t)$  to Eqs. (1)–(5), let  $S_d^u$  be in the set  $U^h$ , and consider the perturbation  $S_d^u(0) \rightarrow 1$  (from  $S_d^u(0) = 0$ ). For a new extra launch of a spacecraft without deorbit capability, we simply set  $S_n(0) \rightarrow S_n(0) + 1$  because an operational spacecraft whose loss does not count as an operational loss can be considered inoperational from the very start.

The legacy cost is the difference between the damage in the current environment and the damage in an environment in which there are no nonoperational hazardous objects; i.e., we use the perturbation  $F_\tau^k(0) \rightarrow 0$ ,  $S_n(0) \rightarrow 0$ , and  $R(0) \rightarrow 0$ . In addition, we assess the portion of the legacy cost due to the FengYun 1C ASAT test via the perturbation  $F_S^h(0) \rightarrow F_S^h(0) - 149.1$  and  $F_S^b(0) \rightarrow F_S^b(0) - 251.8$  (Section F).

The damage generated by a perturbation lasts for  $\approx 10^4$  years, and hence  $n_d^+(T) - n_d^-(T)$  approaches a constant as  $T \rightarrow \infty$  (Fig. 6). In the short term, a breakup produces more damage than an intact of the same type (Fig. 6); in the long term, the opposite is true because an intact remains in orbit longer than a fragment and so is hazardous for longer. In keeping with the sustainability philosophy (long time horizons are also considered for the nuclear waste depository at Yucca Mountain, which needs to comply for  $10^4$  years (Long and Ewing, 2004)), we consider an infinite horizon and refer to the asymptotic value of  $n_d^+(T) - n_d^-(T)$  as the damage. The damage from launching a spacecraft with deorbit capability is  $2.15 \times 10^{-5}$  destroyed spacecraft, which is 3000-fold less damaging than launching a spacecraft without deorbit capability. The FengYun 1C ASAT test can be expected to cause the same damage as 8 rocket body insertions or 2.6 launches of spacecraft that

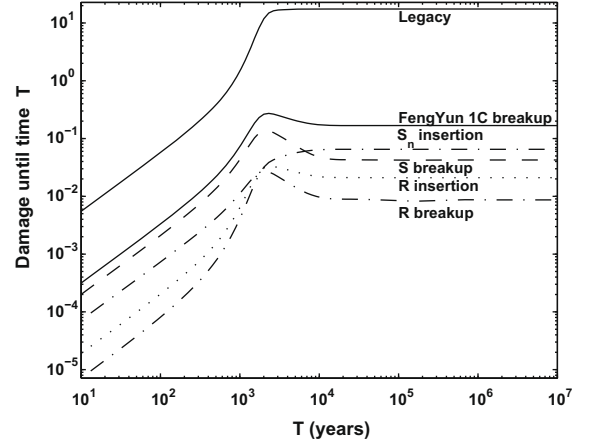


Fig. 6. The damage (i.e., destroyed operational spacecraft) up until time  $T$  caused by various activities that occur at time 0. Some curves have been rendered in different line styles to increase clarity at the intersections.

do not deorbit, and constitutes 1.0% of the total legacy damage. In contrast, as a near-term practical problem, the ASAT test can be expected to cause the same damage over the next 100 years as 16.3 rocket body insertions or 41.1 launches of a spacecraft that does not deorbit, and is 5.8% of the total legacy damage.

Our damage calculations assume that the deorbit compliance rate  $\theta_d$  and the launch rate  $\lambda_o$  do not change in the future. If there is a general consensus in how these parameters might change over time (e.g.,  $\theta_d$  increases from its current rate to a rate where the only noncompliance is due to propulsion system failures), then these predictions could be incorporated into the calculations. With the exception of rocket body breakups, the damage of the various activities varies by <12% for any deorbit compliance rate  $\theta_d \in [0, 0.94]$ . Complex interaction effects make damage calculations sensitive to  $\theta_d$  for  $\theta_d > 0.94$ .

### 3.5. Allocating the legacy damage

Finally, we consider the problem of attributing the total legacy damage to the various responsible parties (e.g., countries). Let  $\rho_{ij}$  be the proportion of objects of type  $\gamma \in U^h$  having party  $i$  as their origin; we are not aware of any fragmentation event in which an object from one nation has been fragmented by an object from another, which allows us to assume that all fragments from an object owned by party  $i$  should be attributed to it. As usual, let  $\gamma$  itself be the number of objects of type  $\gamma$ . Finally, let  $\omega_\gamma$  be the relative hazard of an object of type  $\gamma$ . The proportion of the total hazard that a party's objects contribute is  $h_i \equiv \sum_{\gamma \in U^h} \omega_\gamma \rho_{ij}$ , and the absolute hazard attributed to party  $i$  is  $h_i L$ , where  $L$  is the total legacy damage.

The proportions  $\rho_{ij}$  must be determined by careful analysis of the present catalog, which is beyond the scope of this study. The relative hazard  $\omega_\gamma = \frac{\tilde{\omega}_\gamma}{\sum_\gamma \tilde{\omega}_\gamma}$ , where the hazard  $\tilde{\omega}_\gamma$  is a physical property of a particular object type  $\gamma$

relative to the current orbital environment, and can be calculated as the partial derivative of the damage  $n_d$  with respect to an object type  $\gamma$ :

$$\tilde{\omega}_\gamma = \frac{\partial n_d}{\partial \gamma} \approx \frac{n_d(\gamma + \delta_\gamma) - n_d(\gamma)}{\delta_\gamma}, \quad (17)$$

where the argument of  $n_d$  indicates what is varied. We set the perturbation  $\delta_\gamma = 1$  (although the results are insensitive to  $\delta_\gamma$ ; 0.01 and 1 produce essentially the same hazards), so that  $\tilde{\omega}_\gamma$  coincides with the quantity  $n_d^+ - n_d^-$  defined earlier. We consider an infinite horizon and find that the relative hazard is 0.239 for rocket bodies, 0.739 for spacecraft that do not deorbit, 0.009 for hazardous rocket body fragments, and 0.013 for hazardous spacecraft fragments. Using the initial conditions in Section F and these values, we find that 22.7%, 75.7%, 0.5%, and 1.1% of the total legacy damage is due to intact rocket bodies, intact spacecraft, hazardous rocket body fragments, and hazardous spacecraft fragments, respectively.

## 4. Discussion

### 4.1. The model

Eqs. (1)–(5) attempt to capture the mean behavior of a three-dimensional object-by-object simulation such as LEGEND (Liou et al., 2004) and two-dimensional models of similar complexity (e.g., SDM in (Rossi et al., 1998)). Compared to most previous ODE models (Farinella and Cordelli, 1991; Kessler, 2000; Rossi et al., 1994) (a notable exception is STAT in (Rossi et al., 1998), which considers a large number of ODEs, one for each triple of semimajor axis, eccentricity, and satellite mass), ours is distinctive in that we estimate parameters by taking expectations of empirical distributions, we introduce separate tracking of hazardous and benign fragments, which makes sense given their different mean characteristics, and we introduce the nonuniformity factor that captures the higher collision rates near the poles. Although our model appears at first glance to be much simpler than the simulation model in (Liou et al., 2004), its complexity is in calculating parameter values, which are expectations over the same distributions that govern an object-by-object simulation. The advantages of our approach are enumerated below.

A comparison to results in Liou and Johnson (2008) (which uses LEGEND) shows that our model generates qualitatively similar results (Fig. 1 and Table 1), although any number of physical phenomena and simple accounting differences could explain the discrepancies. These include: differences in assumed characteristics of intact spacecraft and rocket bodies (we assume all spacecraft and rocket bodies have the same mass and take the average area and mass of a satellite from Kessler (2000) because Liou and Johnson (2008) does not provide the relevant quantities); different initial conditions (our knowledge of the initial

conditions used in Liou and Johnson (2008) is quite limited); we use mean values to determine the effects of collisions, whereas each collision in Liou and Johnson (2008) is different; the cost of neglecting fragments from fragmentation events occurring outside the SOI – though fragments from above decay slowly, eccentric fragments would immediately enter the SOI; the error made in assuming that intact–intact collisions occur according to a chemical kinetics model (in particular, intact may have been originally placed in nonconflicting orbits, whereas the chemical kinetics model assumes a particle is placed in a trajectory independent of the positions of any of the other particles); different orbital decay behavior; and rocket bodies are allowed to explode during the first 10 years of the simulation in Liou and Johnson (2008).

There are several advantages to using a simple ODE model such as Eqs. (1)–(5) rather than a complex simulation model: it runs almost instantaneously, which elucidates asymptotic behavior (Kessler, 2000) (this is particularly important given our sustainability framework, which requires an analysis over an infinite time horizon) and eases the sensitivity analysis task (once the parameters are calculated, one can quickly compute many derived quantities that depend on perturbations in mean behavior, whereas it would be necessary to run a computationally intensive object-by-object simulation repeatedly to obtain mean behavior, and then repeat this for each desired perturbation); it allows a level of transparency and understanding that could be valuable if, e.g., multiple countries need to coalesce around a set of damage estimates; and it is amenable to rigorous analytical results involving asymptotic behavior. Our model is generic and can be used at other altitudes, although the space discretization may need to be smaller at lower altitudes to account for the higher sensitivity of escape rate with altitude, and it may be less accurate at altitudes that have considerable congestion at shells just above it (unlike the SOI, see Fig. 7 in Liou and Johnson (2008)).

Nonetheless, while our qualitative results are likely to be correct (e.g., the number of fragments remain bounded, the sustainable lifetime risk to an operational spacecraft is on the order of  $10^{-3}$  if there is high postmission deorbit compliance, and the relative values of the damage due to various activities maintain the rankings in Fig. 6), high-fidelity three-dimensional models are required to confirm them. Moreover, the numerical output of our model should be viewed as rough estimates, and more complex models are required to refine the numerical estimates in Figs. 2–6.

### 4.2. Results

Although our model and analysis have some similarities with previous research, and our numerical results appear to be similar to that of previous research, we come to different conclusions, both in terms of analytical results and policy implications. In terms of analysis, results in Kessler (2000) (when expressed in terms of our Eqs. (6) and (7)) claim that  $F(t)$  grows without bound if  $I(t) > \frac{\mu_F}{\delta_{IF}}$ , which is

referred to as the “runaway threshold”. Setting  $\dot{F}(t) = 0$  in Eq. (7) and solving for  $F$  yields,

$$F(I) = \frac{\delta_{II} I^2}{\mu_F - \delta_{IF} I}, \quad (18)$$

which coincides with Eq. (3) in Kessler (2000). The discrepancy between our claim that  $F(t)$  is always bounded and the result in Kessler (2000) is that the number of intact  $I$  in the numerator of Eq. (18) is treated as a constant in Kessler (2000), whereas we capture via Eq. (6) the dynamic interaction between  $I$  and  $F$  (i.e., intact decrease as fragments increase).

More importantly, while our numerical results mimic earlier results (Liou and Johnson, 2005; Walker and Martin, 2004) that stressed the importance of postmission deorbiting, we do not necessarily agree with the claim that the only way to prevent future problems is to remove existing large intact from space (Liou and Johnson, 2006, 2008). The divergence between our views and those in Liou and Johnson (2006, 2008) is perhaps due to the different performance metrics used. The root causes for alarm in Liou and Johnson (2006, 2008) appear to be the growth rate of fragments and the small increase in the rate of catastrophic collisions over the next 200 years (Liou and Johnson, 2008, Fig. 2). However, the great majority of catastrophic collisions in the SOI do not involve operational spacecraft, and are hazardous only in the sense that the fragments generated from such a collision could subsequently damage or destroy operational spacecraft. Therefore, we introduced the notion of the lifetime risk of an operational spacecraft as the primary performance metric. Our model predicts that the lifetime risk is  $< 5 \times 10^{-4}$  over the next two centuries, and always stays  $< 10^{-3}$  if there is very high ( $> 98\%$ ) spacecraft deorbiting compliance. These risks appear to be low relative to the immense cost and considerable technological uncertainty involved in removing large objects from space, are dwarfed by the  $\approx 20\%$  historical mission-impacting (but not necessarily mission-ending) failure rate of spacecraft (Frost and Sullivan, 2004), and could be overestimated if improved traffic management techniques lower future collision risks (Johnson, 2004). Hence, the need to bring large objects down from space does not appear to be as clear cut as suggested in Liou and Johnson (2006, 2008). Nonetheless, our model does not incorporate the possibility of intentional catastrophic collisions (ASAT tests, space wars) that could conceivably occur in the future. In addition, Fig. 5 considers only catastrophic collisions, whereas noncatastrophic intact-fragment collisions could easily disable an operational spacecraft. If the operational lifetime risk is modified to include noncatastrophic collisions with fragments  $\geq 10\text{cm}$ , then the sustainable risk rises by  $\approx 50\%$ : it increases from  $2.19 \times 10^{-2}$  to  $3.09 \times 10^{-2}$  in the base case, and increases from  $4.91 \times 10^{-4}$  to  $7.94 \times 10^{-4}$  in the full compliance case. Moreover, if fragments  $\geq 1\text{ cm}$  (rather than  $\geq 10\text{ cm}$ )

are harmful to spacecraft (Johnson, 2004), then we (as well as other researchers) could be underestimating the risk.

In summary, in the absence of the removal of large objects from space, the sustainable lifetime risks in Figs. 3–5 do not appear to be obviously above or below a tolerable level. Even if these risks are deemed acceptable, it is prudent to invest in research and development for space remediation technologies, which is a topic of current study (Proposal for forming an IAA study group, 2000). However, given the optimality of full deorbit compliance from a societal, sustainable perspective, and the sensitivity of sustainable lifetime risk to postmission deorbit compliance, the primary focus for policymakers should be on increasing compliance, which leads us to a discussion of economic instruments that could be used to address this issue.

#### 4.3. Setting fees

Creating a set of viable economic instruments will be extremely difficult, and requires sustained political negotiations by a large number of actors; here, we simply discuss some of the key challenges that would be faced in transforming the damages in Fig. 6 into specific fees that could be imposed on past and future debris-generating activities. Such fees are consistent with the “polluter pays” principle proposed to address global climate change (Claussen et al., 1998).

At a strategic level, the first challenge is to decide what types of activities to tax, and for what reasons. One reason to charge a fee is to deter future debris-generating activity (i.e., ideally no fees are collected for certain activities), while another reason could be to generate funds for, e.g., compensating owners of operational spacecraft that are victims of future catastrophic collisions (which are largely random events), subsidizing postmission deorbiting, or performing research and development into various mitigation technologies (e.g., methods that remove large objects from space, electric propulsion systems that could reduce the cost of deorbiting (Ryden et al., 1997), improved space traffic management techniques (Johnson, 2004), and spacecraft shielding).

We begin with the most benign activity, which is the launching of a spacecraft that deorbits after its mission. Because this spacecraft is doing its best to preserve space, one might argue that it should only be charged a fee that compensates for its future expected damage. In this case, the damage that occurs at time  $t$  should be multiplied by  $e^{-rt}$  inside the integral in Eq. (16), where  $r$  is the discount rate, and the total discounted damage should be multiplied by the replacement cost of a satellite. As an illustrative example, if we set  $r = 0.05$  (Perman et al., 2003) and  $C_S = \$0.5\text{B}$ , then the launch fee is only \\$980 (for implementation, the values of  $r$  and  $C_S$  need to be estimated with considerable care and achieve broad consensus).

Note that a noncompliance fee for spacecraft that do not deorbit can be viewed as using differential launch fees

that depend on whether or not a spacecraft deorbits. The primary motivation of a noncompliance fee is to preserve space (Fig. 5). To produce a deterrent effect, the fee to launch a spacecraft that does not deorbit needs to be at least the deorbit cost plus the fee (if any) to launch a spacecraft that deorbits. The voluntary guideline, which implies that it is better to incur a deorbit cost now rather than destroy 0.065 spacecraft in the future, according to our calculations, has not achieved full compliance. It is important to understand the reasons for the current deorbit noncompliance, which could shed light on how to improve compliance. If players are acting rationally and in their own self-interest, then possible reasons for not deorbiting are (i) they are behaving myopically and are discounting collisions that happen far in the future, perhaps having faith in a future technological solution to the problem; (ii) they do not plan many future launches in congested regions of space (such as the SOI), and so will not receive the benefits (i.e., avoided future collisions) from deorbiting; and (iii) they have an inventory of old spacecraft that are expensive to retrofit for deorbiting. To the extent that different players have different (perceived) deorbit costs and benefits, the noncompliance fee (or deorbit subsidy) needs to be sufficiently high to deter all players. If the fee is to be based on damages and if a single player (i.e., space agency) can substantially alter  $\theta_d$  by his postmission deorbit policy, then it may be more appropriate to assess the damage of his aggregate policy decision.

Another challenge for a noncompliance fee stems from the moral hazard issue: the failure rate of propulsion systems has been estimated to be 3.9% (de Weck et al., 2003, Fig. 8) and hence even if a spacecraft owner plans to deorbit after the mission is complete, he may fail to do so, and the international space community may have no way of verifying whether the failure to deorbit was deliberate or unintentional.

The fee structure would have to address this issue. Much of the above discussion about a deorbit noncompliance fee also holds for failing to deorbit rocket bodies or failing to follow passivation techniques, although compliance for these activities in the SOI appears to be much closer to 100% than spacecraft deorbiting.

There is also a legacy issue, which typically arises when discussing launch costs (e.g., Prasad, 2005), in that most of the satellites in LEO were launched by a small group of countries. Hence, there could also be a one-time legacy fee due to all existing space objects currently in the SOI. The use of legacy fees is a particularly thorny political issue related to, e.g., the Cold War and the original research and development costs incurred by the U.S. and U.S.S.R. that subsequent countries did not bear. Sustainability is a modern goal and during the Cold War (when much of the existing debris was generated), the U.S. and U.S.S.R. were not concerned with preserving space for the future. It is also not clear to what extent Russia feels responsible for past U.S.S.R. behavior. In any case, these activities are in the past and not deterable. If one wanted to charge a one-time legacy cost

to cover future expected damages, then (using  $r = 0.05$  and  $C_S = \$0.5B$ ) the legacy fee is \$5.55M, which is negligible compared to the annual budgets of the U.S. and Russian space programs. To allocate this fee across various players, the relative hazards ( $\tilde{\omega}_j$ ) should also be computed with  $r = 0.05$ , which yields 0.618 for rocket bodies, 0.236 for spacecraft that do not deorbit, 0.077 for hazardous rocket body fragments, and 0.068 for hazardous spacecraft fragments; combining these numbers with the initial conditions, we find that the total legacy damage due to these four satellite types is 63.0%, 26.0%, 4.6%, and 6.4%, respectively.

ASAT tests are another politically-charged issue. The FengYun 1C ASAT test may have been partially motivated by former U.S. and Soviet ASAT tests and by the U.S. December 2001 withdrawal from the Anti-Ballistic Missile treaty. As with a deorbit noncompliance fee, the primary goal of an ASAT test fee would be as a deterrent. In contrast to the case where there is a failure to deorbit, it is difficult to determine the magnitude of a financial deterrent because it is very difficult to put a financial cost on the value (to the tester) of an ASAT test. The ASAT test fee might be set to significantly exceed its damage so as to discourage the militarization of space, essentially charging it not only for its test but for the escalation effect it may have on other players. In any case, a test fee would be very difficult to implement from a political standpoint.

## 5. Conclusions

It appears that if full compliance of the 25-year space-craft deorbiting guidelines can be achieved within the next few decades and no ASATs are used or tested in the future, then the lifetime risk from space debris in the SOI may be sustainable at a tolerable ( $\approx 10^{-3}$ ) level. Hence, the focus of policy should be on achieving full deorbit compliance (including improving the reliability of propulsion systems) and fostering a culture that makes ASAT tests (and use) taboo. Indeed, at the current launch rate of 3/year and a deorbit cost of \$0.5M, the total undiscounted deorbit cost after 1000 years is \$1.5B, which is the cost of launching a single defense spacecraft. It seems improbable that a future technology will be able to clean up space for less cost than launching a single defense spacecraft. Our analysis also provides a framework for setting fees for past and future space activities, but many challenges remain in developing a viable set of economic instruments. Finally, we reiterate that our analytical approach does not produce results that are as accurate as a high-fidelity three-dimensional model (e.g., Liou et al., 2004). Hence, our results need to be confirmed by a more complex model before they can inform major space policy decisions.

## Acknowledgements

This research was supported by the Center for Social Innovation, Graduate School of Business, Stanford

University (L.M.W.) and by a Scott A. and Geraldine D. Macomber Stanford Graduate Fellowship and a National Science Foundation Fellowship (A.M.B.). We thank Jeremy Bulow, Lawrence Goulder, Nicholas Johnson, and Erica Plambeck for helpful conversations, and Nicholas Johnson for sharing the data in Table 1. We also thank one of the reviewers for helpful comments.

## Appendix A

In this appendix, we obtain values for the parameters in Eqs. (1)–(5); a more detailed description of our procedure – sufficient for reproducibility of our results – appears in Section B of Bradley and Wein (2008). The values for the collision rate parameters  $\beta_{xy}$ , the fragment generation parameters  $\delta_{xy}^{tk}$ , and the decay rates  $\mu_x$  are found by physical modeling (Alberty and Silbey, 1997; King-Hele, 1964) and calculations using the empirical probability distributions and formulas describing satellite fragmentation and fragment characteristics developed in Johnson et al. (2001), Kessler (2000), and Rossi et al. (1994). The computational framework for incorporating the data in Johnson et al. (2001) is described in Section B. We estimate the collision rate parameters in Section C, the fragment generation parameters in Section D, the decay rates in Section E, and the initial conditions in Section F.

## Appendix B. Computational framework

Calculations for the collision rates, fragment generation rates and decay rates in Sections C, D and E require integrating over five probability distributions, which are listed in the next paragraph, to obtain expected values. Moreover, for the collision rates and fragment generation rates, we are interested in a weighted mean where we associate two weights with a fragment. The first weight function,  $w_1$ , accounts for the proportion of time the fragment spends in the SOI as well as considerations related to eccentricity and deorbit time. The second weight function,  $w_2$ , quantifies the hazard a fragment poses to an intact, and essentially defines the fragments of interest: those that are hazardous to intacts.

Of the five random variables that we consider, the empirical probability distributions in Johnson et al. (2001) govern three of them:

$$\lambda_c = \log_{10} L_c, \quad \text{where } L_c \text{ is the characteristic length,} \quad (\text{B.1})$$

$$\chi = \log_{10}(A/M), \quad \text{where } A/M \text{ is the area-to-mass ratio,} \quad (\text{B.2})$$

$$v = \log_{10} |\Delta v|, \quad \text{where } \Delta v \text{ is the change in velocity.} \quad (\text{B.3})$$

These distributions depend on whether the fragment ejection event is a collision or an explosion and whether the original intact is a rocket body or a spacecraft. We are

interested only in collisions. We introduce two additional random variables:

$$u, \quad \text{the altitude of the satellite in circular orbit generating the fragments,} \quad (\text{B.4})$$

$$z, \quad \text{the direction of } \Delta v \text{ on the sphere.} \quad (\text{B.5})$$

We use the same symbol for both a random variable and a value drawn from its distribution if the distinction is clear from the context. The characteristic length  $L_c$  in (B.1) has a power law distribution,  $\chi$  in (B.2) is conditioned on  $\lambda_c$  and is a mixture of two Gaussians,  $v$  in (B.3) is conditioned on  $\chi$  and has a normal distribution,  $u$  is independent and uniformly distributed on the interval [900, 1000] km, and  $z$  is independent and uniformly distributed on the sphere. The random vector  $\Omega$  has as elements the five random variables in Eqs. (B.1)–(B.5).

Later in this section, we also use Eq. (9) from Johnson et al. (2001), which states that the average area of a fragment having characteristic length  $L_c$  is

$$A = \alpha L_c^{2+\varepsilon}, \quad (\text{B.6})$$

where  $\alpha = 0.556945$  and  $\varepsilon = 0.0047077$ . Rather than view  $A$  as a conditional expectation given a value of  $L_c$ , we treat Eq. (B.6) as a deterministic mapping from the realization of a random characteristic length  $L_c$  to a realization of a random area  $A$ . Similarly, a fragment that is randomly assigned the value  $\chi$  from Eq. (B.2) has a random mass  $m$  given by

$$m = \frac{A}{10^\chi}, \quad (\text{B.7})$$

where  $A$  is the area in Eq. (B.6). That is, a fragment's mass is determined by its characteristic length and its  $A/M$  ratio via Eqs. (B.1), (B.2), (B.6), and (B.7).

The remainder of this section is organized as follows: the proportion of time a fragment spends in the SOI is calculated in Section B.1 and the probability a collision is catastrophic is given in Section B.2; these two calculations form the basis of our weights  $w_1$  and  $w_2$ , respectively. Finally, the expectation of a generic function of the random vector  $\Omega$  is given in Section B.3.

### B.1. The fraction of time spent in the SOI

We use classical orbital mechanics equations (in particular, Eqs. (3.3), (3.10), (3.17), and (3.20) in King-Hele (1964)) and integrate the equations of motion to determine the fraction of time each fragment (whose properties have been sampled via Eqs. (B.1)–(B.5)) spends in the SOI (see Section B.1.1 of Bradley and Wein (2008) for details); each intact in our model is assumed to be in a circular orbit.

The weight  $w_1$  (introduced in Section B) is defined to be the calculated fraction of time spent in the SOI, which varies according to the fragment's properties in Eqs. (B.1)–

(B.5). We also use this calculation of  $w_1$  to help determine the launch rate and the initial number of intact.

As an aside, we conclude this subsection by performing a calculation (similar to one in Rossi (2002)) that is required in Section 3.3: to determine the change in velocity necessary to deorbit an intact from the SOI. We assume the intact has an area-to-mass ratio of  $0.01 \text{ m}^2/\text{kg}$  (Kaula, 1983) and does not deploy an end-of-life sail-like device to increase this ratio. The intact is initially in a circular orbit at 950 km and its initial velocity is 7.375 km/s (Eq. (3.17) in King-Hele (1964)). Fig. 6-2 of NASA Safety Standard 1740.14 (1995) gives orbits as (perigee, apogee) pairs for various area-to-mass ratios that decay naturally in 25 years. We shall be interested in two pairs: (500, 950) and (510, 900).

By considering an apogee of 950 km and a perigee of 500 km, we find that the method that simply lowers the perigee to 500 km requires a speed at apogee of 7.257 km/s. Hence, the required change in velocity is  $\Delta v = 118 \text{ m/s}$ . A second method first lowers the perigee to 510 km and then lowers the apogee to 900 km, and requires  $\Delta v = 128 \text{ m/s}$ . The first method lets the spacecraft linger in the SOI for a little while; the second method shows that only 10.8% more fuel lets the spacecraft leave the SOI essentially immediately. Our model – by assuming all deorbit-capable spacecraft are operational and without providing a nonoperational deorbit state – implicitly assumes the second method is used, although our estimate in the main text of the deorbit cost as a function of  $\Delta v$  is too crude to distinguish between the two methods.

## B.2. The probability a collision is catastrophic

In the model in Johnson et al. (2001), whether a collision is catastrophic depends on the relative velocity and masses of the objects. Because we assume that rocket bodies and spacecraft have the same mass, a particular projectile is hazardous to these two satellites with equal probability.

Fig. 9 of Johnson et al. (2001) presents, for altitudes of 200, 500, 1000, and 1500 km, a piecewise-linear probability density function  $f_{v_c}(v_c)$  of the relative velocity of two objects given that they collide (i.e., the *relative collision velocity*). We use the distribution for the altitude 1000 km, and hence the result is slightly conservative relative to what we would obtain using a distribution for the altitude 950 km, which is the center of our SOI. This distribution implies that the mean relative collision velocity is

$$\bar{v}_c \equiv E[v_c] \approx 12.1 \text{ km/s}, \quad (\text{B.8})$$

which we shall need later.

Let two colliding objects have masses  $m_1$  and  $m_2 \geq m_1$  (in kg). According to Johnson et al. (2001), the collision is catastrophic if the kinetic energy of the projectile in Joules is 40 times greater than the mass of the target in grams. Hence, there is a critical velocity depending on  $m_1$  and  $m_2$ , which we denote by  $v_{\text{crit}}(m_1, m_2)$ , such that

$v_c \geq v_{\text{crit}}(m_1, m_2)$  results in a catastrophic collision. Then the probability the collision is catastrophic is

$$p_c(m_1, m_2) = \int_{v_{\text{crit}}(m_1, m_2)}^{\infty} f_{v_c}(v) dv. \quad (\text{B.9})$$

A fragment's  $w_2$  weight is the probability that an intact-fragment collision involving the given fragment will be catastrophic. Kessler (2000) assumes that any combination of two intact have mass 1600 kg, and we assume that every intact has a mass of  $\hat{M} = 800 \text{ kg}$ . In our simulation model, each fragment is assigned a random mass via Eq. (B.7). A hazardous fragment ( $F_\tau^h$ ) with mass  $m$  has weight  $w_2 = p_c(m, \hat{M})$ , and a benign fragment ( $F_\tau^b$ ) with mass  $m$  has weight  $w_2 = 1 - p_c(m, \hat{M})$ , where  $p_c(m, \hat{M})$  is derived from Eq. (B.9). In Section C, we also use Eq. (B.9) to calculate the fractions of intact-intact and fragment-fragment collisions that are catastrophic.

## B.3. Computing expectations

Because  $w_1$  depends on the fragment's orbit, it is a function of  $v$ ,  $u$ , and  $z$  in Eqs. (B.3)–(B.5). Moreover,  $v$  is conditioned on  $\chi$ , and  $\chi$  is conditioned on  $\lambda_c$ . Hence, any expectation involving the weighting function  $w_1$  must integrate over all five probability density functions (PDFs). The weight  $w_2$  is a function of the mass  $m$  and the hazard type  $\kappa \in \{h, b\}$ ; we write  $w_2(\cdot; \kappa)$  to indicate the latter dependence. The mass  $m$  is a function of the area  $A$  and  $\chi$  via Eq. (B.7), and  $A$  is a function of  $\lambda_c$  by Eq. (B.1). Additionally, the PDFs of some of the random variables are parameterized by the source of the fragments (i.e., rocket body or spacecraft).

Let  $f_\Omega(\omega; \tau, \kappa)$  be the PDF of the random vector  $\Omega$  parameterized by the source  $\tau \in U^I$  and the hazard type  $\kappa \in \{h, b\}$ , and define the weights

$$w(\omega; \kappa) \equiv \frac{w_1(\omega) w_2(\omega; \kappa)}{\int w_1(\omega) w_2(\omega; \kappa) d\omega}. \quad (\text{B.10})$$

Consider first a generic function  $g(\omega)$ . The weighted expected value of  $g$  is

$$E_w[g; \tau, \kappa] \equiv \int g(\omega) f_\Omega(\omega; \tau, \kappa) w(\omega; \kappa) d\omega. \quad (\text{B.11})$$

Similarly, consider a generic function  $h(\omega_1, \omega_2)$ , a function of two vectors independently drawn from the distribution  $f_\Omega$ . The weighted expected value of  $h$  is

$$E_{ww}[h; \tau_1, \kappa_1, \tau_2, \kappa_2] \equiv \int h(\omega_1, \omega_2) f_\Omega(\omega_1; \tau_1, \kappa_1) f_\Omega(\omega_2; \tau_2, \kappa_2) w(\omega_1; \kappa_1) w(\omega_2; \kappa_2) d\omega_1 d\omega_2. \quad (\text{B.12})$$

In Sections C, D and E, we compute the collision rates, the fragment generation rates, and the decay rates by substituting specific functions for  $g(\omega)$  and  $h(\omega_1, \omega_2)$  using Eqs. (B.11) and (B.12).

We approximate the expected values in Eqs. (B.11) and (B.12) by sampling the random vector  $\Omega$  repeatedly and

computing the sample weighted mean of the function at each sample point; details can be found in Section B.1.3 of Bradley and Wein (2008).

## Appendix C. Collision rate parameters

We derive an analytical expression for the collision rate parameter  $\beta$  in Section C.1, estimate the parameter values in this analytical expression in Section C.2, and incorporate nonuniform spatial density in the SOI in Section C.3.

### C.1. Collisions between spherical objects

We assume satellite collisions can be modeled by the ideal-gas model in chemical kinetics (Alberty and Silbey, 1997). Consider two spheres contained in a large volume  $V$  having random radii  $r_1$  and  $r_2$ , and random relative speed  $v_{12} \sim f_{v_{12}}(v)$ . They collide if their centers are within a distance  $d_{12} = r_1 + r_2$ , referred to as the collision diameter, of each other. As in Johnson et al. (2001) and Kessler (2000), we use the collision cross section  $\sigma_{12}$  rather than the collision diameter  $d_{12}$ , where  $\sigma_{12} = \pi d_{12}^2$ . Let  $\bar{v}_{12} \equiv \int v_{12} f_{v_{12}}(v) dv$  be the *collision probability velocity*. It follows (see Section B.2.1 of Bradley and Wein (2008) for details) from Eqs. (1)–(5) that the parameter  $\beta$  corresponds to  $\tilde{\beta} \equiv \frac{\bar{v}_{12}}{V} E[\sigma_{12}]$ .

Finally, while the  $w_2$  weights in Section B.2 quantify the fraction of intact-fragment collisions that are catastrophic, we have yet to account for the fraction of intact-intact and fragment-fragment collisions that are catastrophic. We do so using the variable  $\psi$ , where a proportion  $1 - \psi$  of collisions are disregarded because they are not catastrophic; as shown in Section C.2,  $\psi$  is derived for various intact-intact and fragment-fragment collisions using the probabilities  $p_c(m_1, m_2)$  in Eq. (B.9). Hence, we define the collision rate parameter by

$$\tilde{\beta} \equiv \frac{\bar{v}_{12}}{V} E[\psi \sigma_{12}], \quad (\text{C.1})$$

where the tilde denotes that the spatial density of satellites is assumed to be uniform in the SOI. In Section C.3, we multiply  $\tilde{\beta}$  by a nonuniformity factor to obtain the collision rate parameter  $\beta$ .

### C.2. Estimating parameters in Eq. (C.1)

In this subsection, we estimate the quantities  $V$ ,  $\bar{v}_{12}$ ,  $\sigma_{12}$ , and  $\psi$  in Eq. (C.1). The Earth's radius is 6378 km, and hence the volume of our compartment is  $V = \frac{4}{3}\pi((6378 + 1000)^3 - (6378 - 900)^3) = 6.748 \times 10^{10} \text{ km}^3$ . We take the collision probability velocity to be  $\bar{v}_{12} = 8.8 \text{ km/s}$  (Johnson et al., 2001, Fig. 8).

For  $\alpha, \gamma \in \{U\}$ , we have  $\sqrt{\sigma_{\alpha\gamma}} = \sqrt{\sigma_\alpha} + \sqrt{\sigma_\gamma}$ , and it remains to determine the cross sections  $\sigma_S$ ,  $\sigma_R$ , and  $\sigma_{F_t^\kappa}$ . In his calculations, Kessler (Kessler, 2000) assumes that the collision cross section of a fragment is zero; hence his cross section values are for intacts only. We do not know the

individual cross sections of spacecraft or rocket bodies and so must use average values to obtain  $\sigma_S$  and  $\sigma_R$ . Kessler obtains average cross sections for the region [920, 1020] km of  $\sigma_f = 14.1 \text{ m}^2$  for intact-fragment collisions and  $\sigma_i = 53.8 \text{ m}^2$  for intact-intact collisions (Kessler, 2000). The ratio  $\sigma_i/\sigma_f = 3.82 < 4$  (by less than 5 %) because  $\sigma_i$  is computed by averaging over all intact-intact combinations in his database. Our calculations assume the ratio is exactly 4, effectively using only the  $14.1 \text{ m}^2$  value. Kessler observes that spacecraft have an average cross section 0.35 times the average, or  $\sigma_S = 0.35 \times 14.1 = 4.94 \text{ m}^2$ , and rocket bodies have an average cross section  $\sigma_R = 1.65 \times 14.1 = 23.3 \text{ m}^2$  (Kessler, 2000).

For fragments, we have a probability distribution over the area  $A$  from Eq. (B.6), which corresponds to the cross section under the assumption that fragments are spherical. Under this assumption, the collision cross section for an intact and fragment is

$$\sigma_{\alpha F_t^\kappa} = \left( \sqrt{\sigma_\alpha} + \sqrt{A} \right)^2, \quad (\text{C.2})$$

and the collision cross section for two fragments is

$$\sigma_{F_{\tau_1}^{\kappa_1} F_{\tau_2}^{\kappa_2}} = \left( \sqrt{A_1} + \sqrt{A_2} \right)^2. \quad (\text{C.3})$$

The final parameters to estimate are the catastrophic probabilities  $\psi$ . The change over time of the proportion of fragments that are hazardous to intacts is accounted for by the separate hazardous and benign fragment types and corresponding equations in Eqs. (1)–(5) and the  $w_2$  weights in Section B.2. Therefore, all intact-fragment collisions are counted and we set  $\psi_{\alpha F_t^\kappa} = 1$  for  $\alpha \in U^I$ .

All intacts have the same mass,  $\hat{M} = 800 \text{ kg}$ . Therefore, each poses the same threat to the others, and Eq. (B.9) implies that

$$\psi_I \equiv \psi_{\alpha\gamma} = p_c(\hat{M}, \hat{M}) = 0.9996 \quad \text{for } \alpha, \gamma \in U^I; \quad (\text{C.4})$$

i.e., nearly all intact-intact collisions are catastrophic.

Fragments pose different hazards to each other. By Eq. (B.9), the probability that a collision between a fragment of type  $F_{\tau_1}^{\kappa_1}$  with mass  $m_1$  and one of type  $F_{\tau_2}^{\kappa_2}$  with mass  $m_2$  is catastrophic is

$$\psi_{F_{\tau_1}^{\kappa_1} F_{\tau_2}^{\kappa_2}} = p_c(m_1, m_2). \quad (\text{C.5})$$

For all types of fragment-fragment collisions,  $\psi > 0.96$  when averaged over  $\Omega$ .

Though Johnson et al. (2001) defines a noncatastrophic collision as one in which only the less massive object breaks up, we assume that in intact-intact and fragment-fragment collisions, a noncatastrophic collision produces no new fragments. Because essentially all intact-intact and almost all fragment-fragment collisions are catastrophic, there is little error in making this assumption, and the error is conservative. As in Johnson et al. (2001), we assume that only the less massive object breaks up in noncatastrophic intact-fragment collisions.

The value of  $\tilde{\beta}$  is obtained by taking the expectation in Eq. (C.1) and substituting Eqs. (C.2)–(C.5) for the generic functions in Eqs. (B.11) and (B.12). For intact–intact collisions, Eq. (C.1) contains no random variables and we have

$$\tilde{\beta}_{xy} = \frac{\bar{v}_{12}}{V} \psi_I \sigma_{xy} \quad \text{for } x, y \in U^I, \quad (\text{C.6})$$

where  $\psi_I$  is given in Eq. (C.4). For intact–fragment collisions, we have

$$\tilde{\beta}_{xF_i^k} = \frac{\bar{v}_{12}}{V} E_w [\sigma_{xF_i^k}; \tau, \kappa], \quad (\text{C.7})$$

and for fragment–fragment collisions, we have

$$\tilde{\beta}_{F_{\tau_1}^{\kappa_1} F_{\tau_2}^{\kappa_2}} = \frac{\bar{v}_{12}}{V} E_{ww} [\psi_{F_{\tau_1}^{\kappa_1} F_{\tau_2}^{\kappa_2}} \sigma_{F_{\tau_1}^{\kappa_1} F_{\tau_2}^{\kappa_2}}; \tau_1, \kappa_1, \tau_2, \kappa_2]. \quad (\text{C.8})$$

The numerical values from Eqs. (C.6)–(C.8) for both versions of the model (i.e., in the absence and presence of fragment–fragment collisions) appear in Tables C.1 and C.2.

### C.3. Nonuniform spatial density

Satellites are distributed nonuniformly throughout the SOI for two reasons: a satellite having an approximately

circular orbit tends to spend a greater proportion of time at latitudes near its inclination than at other latitudes, and the volume of the SOI as a function of latitude decreases near the poles. We incorporate these phenomena into our model by considering a nonuniform version of the ideal gas model.

Consider populations of two types of spherical objects mixed homogeneously in a region of space having volume  $V$ . Each population has number density  $\rho_i \equiv \frac{n_i}{V}, i = 1, 2$ . The ideal gas model gives the number of collisions  $c$  in a unit of time as

$$c = b_{12} V \rho_1 \rho_2 = b_{12} \frac{n_1 n_2}{V} \quad (\text{C.9})$$

for some constant  $b_{12}$ .

Suppose the objects prefer some parts of space over others. Break the region into voxels indexed by  $j$ , each having volume  $V_j$ . Let the objects of type  $i$  have number density  $n_i \rho_{ij}$  in voxel  $j$ . Eq. (C.9) holds in each voxel  $j$ ; summing over the voxels yields  $c = b_{12} n_1 n_2 \sum_j V_j \rho_{1j} \rho_{2j} = f_{12} b_{12} \frac{n_1 n_2}{V}$ , where we define

$$f_{12} \equiv V \sum_j V_j \rho_{1j} \rho_{2j} \quad (\text{C.10})$$

Table C.1

Parameter values for Eqs. (1)–(5), where time is in years. In each of the five sections of the table, the parameter is given in the far left column, the rows are the first subscript, the columns are the second subscript, and the table entries are the parameter values; e.g., the second row, fifth column of the second section yields  $\delta_{SF_R^h}^{Rh}/\beta_{SF_R^h} = -1.00$ .

	<i>R</i>	<i>S</i>	$F_R^h$	$F_R^b$	$F_S^h$	$F_S^b$
$\beta$	<i>R</i>	2.55e-7	1.36e-7	7.64e-8	6.70e-8	7.18e-8
	<i>S</i>		5.42e-8	2.02e-8	1.51e-8	1.77e-8
	$F_R^h$			3.67e-9	1.17e-9	2.58e-9
	$F_R^b$				1.86e-10	6.30e-10
	$F_S^h$					1.66e-9
	$F_S^b$					1.64e-10
$\frac{\delta^{Rh}}{\beta}$	<i>R</i>	75.57	37.78	43.76	0	44.79
	<i>S</i>		0	-1.00	0	0
	$F_R^h$			0	0	0
	$F_R^b$				0	0
	$F_S^h$				0	0
	$F_S^b$					0
$\frac{\delta^{Rb}}{\beta}$	<i>R</i>	279.73	139.87	165.68	-1.00	165.80
	<i>S</i>		0	0	-1.00	0
	$F_R^h$			0	0	0
	$F_R^b$				0	0
	$F_S^h$				0	0
	$F_S^b$					0
$\frac{\delta^{Sh}}{\beta}$	<i>R</i>	0	98.19	0	0	-1.00
	<i>S</i>		196.38	115.99	0	115.21
	$F_R^h$			0	0	0
	$F_R^b$				0	0
	$F_S^h$				0	0
	$F_S^b$					0
$\frac{\delta^{Sb}}{\beta}$	<i>R</i>	0	165.64	0	0	-1.00
	<i>S</i>		331.29	195.66	0	196.04
	$F_R^h$			0	0	0
	$F_R^b$				0	0
	$F_S^h$				0	0
	$F_S^b$					0

Table C.2

Parameter values for the fragment–fragment version of Eqs. (1)–(5). See the legend to Table C.1 for an explanation.

	$R$	$S$	$F_R^h$	$F_R^b$	$F_S^h$	$F_S^b$
$\tilde{\beta}$	$R$	2.55e-7	1.36e-7	7.64e-8	6.70e-8	7.18e-8
	$S$		5.42e-8	2.02e-8	1.51e-8	1.77e-8
	$F_R^h$			3.64e-9	1.17e-9	2.59e-9
	$F_R^b$				1.86e-10	6.29e-10
	$F_S^h$					1.66e-9
	$F_S^b$					6.67e-10
$\frac{\delta^{Rh}}{\beta}$	$R$	75.57	37.78	44.54	0	44.79
	$S$		0	0.36	0	0
	$F_R^h$			7.98	3.59	5.30
	$F_R^b$				0	0
	$F_S^h$				0	0
	$F_S^b$					0
$\frac{\delta^{Rb}}{\beta}$	$R$	279.73	139.87	168.57	-0.79	165.80
	$S$		0	5.03	-0.78	0
	$F_R^h$			36.93	16.77	23.32
	$F_R^b$				1.85	-0.07
	$F_S^h$					1.03
	$F_S^b$					0
$\frac{\delta^{Sh}}{\beta}$	$R$	0	98.19	0	0	0.62
	$S$		196.38	115.99	0	117.67
	$F_R^h$			0	0	8.24
	$F_R^b$				0	9.59
	$F_S^h$					22.62
	$F_S^b$					11.53
$\frac{\delta^{Sb}}{\beta}$	$R$	0	165.64	0	0	2.73
	$S$		331.29	195.66	0	200.19
	$F_R^h$			0	0	15.58
	$F_R^b$				0	17.87
	$F_S^h$					41.53
	$F_S^b$					21.27

to be the nonuniformity factor. If the density is uniform, then  $n_i \rho_{ij} = \frac{n_i}{V}$  and hence  $f_{12} = 1$ .

We assume that the density  $\rho_{ij}$  is constant in time, so that  $c(t) = f_{12} b_{12} n_1(t) n_2(t)/V$  for all  $t \geq 0$ . Hence, we can accommodate spatial nonuniformity in our ODE model by simply multiplying the rate  $\tilde{\beta}$  by the nonuniformity factor. More specifically, in the remainder of this section we calculate  $f_{\alpha\gamma}$  for  $\alpha, \gamma \in \{R, S, F\}$ , which allows us to use Eqs. (C.6)–(C.8) to define the collision rate parameters

$$\beta_{\alpha\gamma} = f_{\alpha\gamma} \tilde{\beta}_{\alpha\gamma} \quad \text{for } \alpha, \gamma \in U^I, \quad (\text{C.11})$$

$$\beta_{\alpha F_i^k} = f_{\alpha F_i^k} \tilde{\beta}_{\alpha F_i^k} \quad \text{for } \alpha \in U^I, \quad (\text{C.12})$$

$$\beta_{F_{i_1}^{k_1} F_{i_2}^{k_2}} = f_{FF} \tilde{\beta}_{F_{i_1}^{k_1} F_{i_2}^{k_2}}. \quad (\text{C.13})$$

We discretize SOI into 90 voxels, where voxel  $j \in \{1, 2, \dots, 90\}$  spans the latitudes  $(j-1)^\circ$  to  $j^\circ$ , so that the volume of voxel  $j$  is

$$V_j = \int_{\frac{\pi}{2} + \frac{(j-1)\pi}{180}}^{\frac{\pi}{2} + \frac{j\pi}{180}} \int_{R_e + 900}^{R_e + 1000} \int_0^{2\pi} r^2 \sin \phi \, d\theta \, dr \, d\phi. \quad (\text{C.14})$$

For each fragment, rocket body, and spacecraft in the current publicly available catalog (Space Track, 2008), we use the method described in Section B.1 to calculate the proportion of time the satellite spends in the SOI in each lati-

Table C.3

The nonuniformity parameters  $f_{\alpha\gamma}$  derived in Section C.3. The rows correspond to the first subscript and the columns correspond to the second subscript; e.g.,  $f_{FR} = 1.39$ .

$f$	$F$	$R$	$S$
$F$	1.38	1.39	1.33
$R$		1.72	1.55
$S$			1.44

tude bin (see Section B.2.3 of Bradley and Wein (2008) for details), which allows us to determine the densities  $\rho_{ij}$ . The nonuniformity factors  $f_{\alpha\gamma}$  are calculated via Eq. (C.10) and appear in Table C.3. An analysis of the catalog shows that there are a large number of SL-8 rocket bodies having inclinations between  $82^\circ$  and  $83^\circ$ ; their presence is the primary reason why  $f_{R\gamma}$  is larger than the other nonuniformity factors.

#### Appendix D. Debris generation parameters

In this section, we derive an expression for the debris generation parameter. Suppose that in addition to a radius  $R$ , a sphere has a mass  $M$ , and that the random variables  $(R, M) \equiv \tilde{\Omega} \sim f_{\tilde{\Omega}}(\tilde{\omega})$ . Colliding spheres break up to pro-

duce fragments. A collision between spheres 1 and 2 generates  $\hat{N}(m_1, m_2)$  fragments. Then the expected number of fragments generated per unit time is

$$\frac{1}{2} \frac{N^2 \pi \bar{v}_{12}}{V} \int \hat{N}(m_1, m_2) (r_1 + r_2)^2 f_{\tilde{\Omega}}(\tilde{\omega}_1) f_{\tilde{\Omega}}(\tilde{\omega}_2) d\tilde{\omega}_1 d\tilde{\omega}_2. \quad (\text{D.1})$$

By Eqs. (1)–(5), we see that the debris generation parameter  $\delta$  corresponds to

$$\frac{\bar{v}_{12}}{V} \int \hat{N}(m_1, m_2) \sigma_{12} f_{\tilde{\Omega}}(\tilde{\omega}_1) f_{\tilde{\Omega}}(\tilde{\omega}_2) d\tilde{\omega}_1 d\tilde{\omega}_2, \quad (\text{D.2})$$

except that Eq. (D.2) does not take into account the variable  $\psi$  (see Eq. (C.1)) and the fact that a fragment's orbit is often only partly in the SOI after a fragmentation event. The expected proportion of time that a fragment – of type  $F_\tau^\kappa$  and produced by an intact of type  $\alpha \in U^I$  or a fragment of type  $F_\alpha^h$  in a catastrophic collision – spends in the SOI is

$$s_\alpha^{\tau\kappa} = \begin{cases} 0 & \text{if } \tau \neq \alpha; \\ \int w_1(\omega) w_2(\omega; \kappa) f_\Omega(\omega; \tau, \kappa) d\omega & \text{if } \tau = \alpha. \end{cases} \quad (\text{D.3})$$

The integral in Eq. (D.3) is the expectation of the product of the weights  $w_1$  and  $w_2$  defined in Sections B.1 and B.2. A benign fragment of type  $F_\alpha^b$  generates only benign fragments and so  $w_2$  is excluded:

$$s_\alpha^{\tau b} = \begin{cases} 0 & \text{if } \tau \neq \alpha; \\ \int w_1(\omega) f_\Omega(\omega; \tau, b) d\omega & \text{if } \tau = \alpha. \end{cases} \quad (\text{D.4})$$

These expectations are independent of what follows because they concern a property of the proportion of fragments generated, which, except for intact source type, is independent of properties of the colliding fragments.

We now define the function  $D_{\alpha\gamma}^{\tau\kappa}$ , which quantifies – for specific fragment property values – the number of fragments emerging from a collision weighted by the fraction of time  $s_\alpha^{\tau\kappa}$  in Eqs. (D.3) and (D.4) that fragments spend in the SOI. Then, by Eq. (D.2), we have

$$D_{\alpha\gamma}^{\tau\kappa} = \frac{\bar{v}_{12}}{V} E \left[ D_{\alpha\gamma}^{\tau\kappa} \psi_{\alpha\gamma} \sigma_{\alpha\gamma} \right]. \quad (\text{D.5})$$

We need the specific power law distribution given in Eq. (4) in Johnson et al. (2001), which states that the number of fragments from a collision having characteristic length at least  $L_c$  m is

$$N(L_c; M) = 0.1 M^{0.75} L_c^{-1.71}, \quad (\text{D.6})$$

where  $M$  is the mass of the objects involved if the collision is catastrophic, and  $M$  is the product of the mass of the less massive object and the relative collision velocity  $v_c$  in a noncatastrophic collision. We are interested only in fragments having  $L_c \geq \hat{L}_c \equiv 10$  cm, and for convenience we define  $\hat{N}(M) \equiv N(\hat{L}_c; M)$ .

Consider a catastrophic collision between two objects of masses  $m_i, i = 1, 2$ . The collision produces  $\hat{N}(m_1 + m_2)$  fragments. We assume – this assumption goes beyond the model in Johnson et al. (2001) – that the proportion of fragments object  $i$  generates is  $\frac{m_i}{m_1 + m_2}, i = 1, 2$ . Each object produces fragments of various types.

We first derive  $D_{\alpha\gamma}^{\tau\kappa}$  for intact–intact collisions. A collision between two intact of types  $\alpha, \gamma \in U^I$  generates

$$D_{\alpha\gamma}^{\tau\kappa} = \frac{\hat{N}(2\hat{M}) (s_\alpha^{\tau\kappa} + s_\gamma^{\tau\kappa})}{2} \quad (\text{D.7})$$

fragments of type  $F_\tau^\kappa$ . In intact–intact collisions,  $D_{\alpha\gamma}^{\tau\kappa}$  and  $\beta_{\alpha\gamma}^{\tau\kappa}$  are independent.

A collision between an intact of type  $\alpha \in U^I$  and a benign fragment of type  $F_\tau^b$  and having mass  $m$  is noncatastrophic; only the benign fragment breaks up. The fragment generates

$$D_{\alpha F_\tau^b}^{\tau b} \equiv \hat{N}(m \bar{v}_c) s_\tau^{\tau b} - 1 \quad (\text{D.8})$$

fragments also of type  $F_\tau^b$ , where we make use of  $\bar{v}_c = 12.1$  km/s from Eq. (B.8). The  $-1$  accounts for the loss of the original fragment.

A catastrophic collision between an intact of type  $\alpha \in U^I$  having mass  $\hat{M}$  and a fragment of type  $F_{\tau_1}^h$  having mass  $m$  generates, by Eqs. (D.2)–(D.4),

$$D_{\alpha F_{\tau_1}^h}^{\tau_2 \kappa} \equiv \hat{N}(\hat{M} + m) \left( \frac{\hat{M}}{\hat{M} + m} s_\alpha^{\tau_2 \kappa} + \frac{m}{\hat{M} + m} s_{\tau_1}^{\tau_2 \kappa} \right) - \delta(\tau_1, \tau_2) \quad (\text{D.9})$$

fragments of type  $F_{\tau_2}^{\kappa}$ , where  $\delta(\tau_1, \tau_2) = 1$  if  $\tau_1 = \tau_2$  and 0 otherwise. The second term in parentheses is neglected in the fragment–fragment version of the model.

Finally, by Eqs. (D.2)–(D.4), a catastrophic collision between two fragments of types  $F_{\tau_1}^{\kappa_1}$  and  $F_{\tau_2}^{\kappa_2}$  generates

$$D_{F_{\tau_1}^{\kappa_1} F_{\tau_2}^{\kappa_2}}^{\tau_3 \kappa_3} \equiv \hat{N}(m_1 + m_2) \left( \frac{m_1}{m_1 + m_2} s_{F_{\tau_1}^{\kappa_1}}^{\tau_3 \kappa_3} + \frac{m_2}{m_1 + m_2} s_{F_{\tau_2}^{\kappa_2}}^{\tau_3 \kappa_3} \right) - \delta(\tau_3, \tau_1) - \delta(\tau_3, \tau_2) \quad (\text{D.10})$$

fragments of type  $F_{\tau_3}^{\kappa_3}$ .

We conclude this subsection by taking the expectation in Eq. (D.5). For an intact–intact collision, the expressions do not have any random variables, and

$$\delta_{\alpha\gamma}^{\tau\kappa} \equiv \frac{\hat{N}(2\hat{M}) (s_\alpha^{\tau\kappa} + s_\gamma^{\tau\kappa}) \bar{v}_{12} \psi_{\alpha\gamma} \sigma_{\alpha\gamma}}{2V}. \quad (\text{D.11})$$

For a collision between an intact and a benign fragment, we have

$$\delta_{\alpha F_\tau^b}^{\tau b} \equiv \frac{\bar{v}_{12} E_w \left[ D_{\alpha F_\tau^b}^{\tau b} \sigma_{\alpha F_\tau^b}; \tau, b \right]}{V}, \quad (\text{D.12})$$

and for a collision between an intact and a hazardous fragment, we have

$$\delta_{\alpha F_{\tau_1}^h}^{\tau_2 \kappa} \equiv \frac{\bar{v}_{12} E_w \left[ D_{\alpha F_{\tau_1}^h}^{\tau_2 \kappa} \sigma_{\alpha F_{\tau_1}^h}; \tau_1, h \right]}{V}. \quad (\text{D.13})$$

Finally, the expectation for a catastrophic collision between two fragments is

Table E.1

The inverse of the decay rates (in years) derived in Section E. The columns correspond to the subscript; e.g.,  $\mu_s^{-1} = 1.10 \times 10^4$ .

$\mu^{-1}$	$R$	$S$	$F_R^h$	$F_R^b$	$F_S^h$	$F_S^b$
	$1.10 \times 10^4$	$1.10 \times 10^4$	$1.23 \times 10^3$	$3.12 \times 10^2$	$2.64 \times 10^3$	$7.57 \times 10^2$

$$\delta_{F_{\tau_1}^{K_1} F_{\tau_2}^{K_2}}^{\tau_3 K_3} = \frac{\bar{v}_{12} E_{ww} \left[ D_{F_{\tau_1}^{K_1} F_{\tau_2}^{K_2}}^{\tau_3 K_3} \psi_{F_{\tau_1}^{K_1} F_{\tau_2}^{K_2}} \sigma_{F_{\tau_1}^{K_1} F_{\tau_2}^{K_2}} ; \tau_1, K_1, \tau_2, K_2 \right]}{V}. \quad (\text{D.14})$$

Although Eqs. (D.11)–(D.14) yield  $\delta_{\alpha}^{\tau_K}$ , we display values for  $\frac{\delta_{\alpha}^{\tau_K}}{\beta_{\alpha}}$ , which is roughly the average number of fragments of a certain type generated by a certain type of collision. These numerical values for both versions of the model appear in Tables C.1 and C.2.

## Appendix E. Decay rates

In this section, we estimate the decay rates for intact without deorbit capability ( $\mu_R$  and  $\mu_n$ ) and fragments ( $\mu_{F_\tau^K}$ ). As noted in the main text, we set  $\mu_o^{-1} = 3$  years for intact with deorbit capability ( $\mu_o$ ). We estimate the decay rates  $\mu_R$ ,  $\mu_n$ , and  $\mu_{F_\tau^K}$  as reciprocals of residence times. Table 4 in Rossi et al. (1994) gives the residence time in years of a satellite in various shells, and the residence time for the SOI is 110 years. The table is calibrated for an A/M ratio of 1 m<sup>2</sup>/kg; the residence time for a satellite having a different value of A/M is obtained by dividing the time by that value.

Recommended values for the A/M ratio for intact range between  $2 \times 10^{-3}$  and  $2 \times 10^{-2}$  m<sup>2</sup>/kg (Kaula, 1983), which yield residence times of between  $5.5 \times 10^3$  and  $5.5 \times 10^4$  years. Either of these values makes the decay rate for intact insignificant in the next few centuries. We use  $\mu_R = \mu_n = \frac{1 \times 10^{-2}}{110} = 9.1 \times 10^{-5}$ /year.

The four fragment types  $F_\tau^K$  have different average A/M values. By Eqs. (B.2) and (B.11), we compute the fragment decay rates via

$$\mu_{F_\tau^K} = \frac{E_w[10^\tau; \tau, \kappa]}{110}. \quad (\text{E.1})$$

The numerical results from Eq. (E.1) appear in Table E.1. Kessler (2000) uses a decay rate of  $\frac{1}{493}$  per year, which is between the four fragment decay rates calculated from Eq. (E.1).

## Appendix F. Initial conditions

In this section, we allocate the total number of initial fragments  $F^s(0)$  among the four fragment types. In Farinella and Cordelli (1991), it is suggested that most fragments are from exploding rocket bodies. We assume 90 % of the initial fragments are from rocket bodies, with one exception that is allocated entirely to a spacecraft source: by separately analyzing the fragment entries in Space Track (2008) that additionally contain the tag “FENGYUN 1C”, we calculate that

400.9 of the 955.5 initial effective fragments in the SOI are from the Chinese ASAT test resulting in the breakup of the FengYun 1C spacecraft, which broke up at  $\approx 850$  km (Liou and Portman, 2007). Though the number 90% is just a guess, the results are insensitive to it; moreover, a smaller proportion from rocket bodies yields a higher fraction of hazardous fragments, and so choosing a high proportion is conservative. Finally, we use the parameters  $s_\alpha^{\tau_K}$  in Eq. (D.3), i.e., the proportion of fragments of type  $F_\tau^K$  generated by the breakup of an intact  $\alpha$ , to determine the mix of hazardous and benign fragments. This is a conservative choice because benign fragments deorbit faster than hazardous ones on average and so if no new breakups occur, the proportion of hazardous fragments increases with time. These allocations result in the initial conditions  $F_S^h(0) = 169.8$ ,  $F_R^h(0) = 106.2$ ,  $F_S^b(0) = 286.5$ , and  $F_R^b(0) = 393.0$ . Using the same procedure, we find that of the 400.9 fragments from the FengYun 1C spacecraft, 149.1 are hazardous and 251.8 are benign.

## References

- Alberty, R.A., Silbey, R.J. Physical Chemistry, second ed John Wiley and Sons, New York, NY, 1997.
- Bradley, A.M., Wein, L.M. Space Debris: Assessing Risk and Responsibility. Graduate School of Business, Stanford University, Stanford, CA, 2008.
- Claussen, E., McNeilly, L. Equity and Global Climate Change: the Complex Elements of Global Fairness. Pew Center on Global Climate Change, October 29, 1998. Accessed at: <[http://www.pewclimate.org/global-warming-in-depth/all\\_reports/equity\\_and\\_climate\\_change](http://www.pewclimate.org/global-warming-in-depth/all_reports/equity_and_climate_change)> (accessed May 20, 1998).
- de Weck, O., de Neufville, R., Chang, D., Chaize, M. Technical Success and Economic Failure. Unit 1 of Communications Satellite Constellations, Engineering Systems Learning Center, MIT, Cambridge, MA, October 14, 2003. Accessed at: <[http://ardent.mit.edu/real\\_options/de%20Weck%20System%20Study/unit1\\_summary.pdf](http://ardent.mit.edu/real_options/de%20Weck%20System%20Study/unit1_summary.pdf)> (accessed June 2, 2008).
- Farinella, P., Cordelli, A. The proliferation of orbiting fragments: a simple mathematical model. Sci. Global Security 2, 365–378, 1991.
- Frost and Sullivan. Commercial Communications Satellite Bus Reliability Analysis, August 2004. Accessed at: <<http://www.satelliteonthenet.co.uk/white/frost3.html>> (accessed June 3, 2008).
- Guidelines and Assessment Procedures for Limiting Orbital Debris, NASA Safety Standard 1740.14, NASA Office of Safety and Mission Assurance, August 1995.
- Johnson, N.L. Space traffic management: concepts and practices. Space Policy 20, 79–85, 2004.
- Johnson, N.L., Krisko, P.H., Liou, J.-C., Anz-Meador, P.D. NASA’s new breakup model of EVOLVE 4.0. Adv. Space Res. 28, 1377–1384, 2001.
- Kaula, W.M. Theory of Satellite Geodesy: Applications of Satellites to Geodesy. Yale University Press, New Haven, CT, 1983.
- Kessler, D.J. Critical Density of Spacecraft in Low Earth Orbit: Using Fragmentation Data to Evaluate the Stability of the Orbital Debris Environment. Johnson Space Center Report No. 28949, NASA and LMSEAT Report No. 33303, Lockheed Martin, February 2000.

- King-Hele, D. Theory of Satellite Orbits in an Atmosphere. Blackie, Glasgow and London, 1964.
- Liou, J.-C., Johnson, N.L. A LEO satellite postmission disposal study using LEGEND. *Acta Astronaut.* 57, 324–329, 2005.
- Liou, J.-C., Johnson, N.L. Risks in space from orbiting debris. *Science* 311, 340–341, 2006.
- Liou, J.-C., Johnson, N.L., A Sensitivity Analysis of the Effectiveness of Active Debris Removal in LEO, Paper IAC-07-A6.3.05. International Astronautical Congress, Hyderabad, India, September 2007. Accessed at: <[http://ntrs.nasa.gov/archive/nasa/casi.ntrs.nasa.gov/20070013702\\_2007011170.pdf](http://ntrs.nasa.gov/archive/nasa/casi.ntrs.nasa.gov/20070013702_2007011170.pdf)> (accessed December 17, 2007).
- Liou, J.-C., Johnson, N.L. Instability of the present LEO satellite populations. *Adv. Space Res.* 41, 1046–1053, 2008.
- Liou, J.-C., Portman, S. Chinese anti-satellite test creates most severe orbital debris cloud in history. *Orbital Debris Quart. News* 11, 2–3, 2007.
- Liou, J.-C., Hall, D.T., Krisko, P.H., Opiela, J.N. LEGEND – a three-dimensional LEO-to-GEO debris evolutionary model. *Adv. Space Res.* 34, 981–986, 2004.
- Long, J.C.S., Ewing, R.C. Yucca Mountain: Earth-science issues at a geologic repository for high-level nuclear waste. *Annu. Rev. Earth Planet. Sci.* 32, 363–401, 2004.
- Perman, R., Ma, Y., McGilvray, J., Common, M. Natural Resource and Environmental Economics, third ed Pearson Education Ltd, Harlow, UK, 2003.
- Prasad, M.Y.S. Technical and legal issues surrounding space debris – India's position in the UN. *Space Policy* 21, 243–249, 2005.
- Proposal for Forming an IAA study group, IAA, Paris, October 2000. Available at: <<http://iaaweb.org/iaa/Scientific%20Activity/Study%20-Groups/SG%20Commission%205/sg55/s55.pdf>> (accessed June 10, 2008)..
- Rossi, A. Energetic cost and viability of the proposed space debris mitigation measures. *J. Spacecraft Rockets* 39, 540–550, 2002.
- Rossi, A., Cordelli, A., Farinella, P., Anselmo, L. Collisional evolution of Earth's orbital debris cloud. *J. Geophys. Res.* 99, 23195–23210, 1994.
- Rossi, A., Anselmo, L., Cordelli, A., Farinella, P., Pardini, C. Modelling the evolution of the space debris population. *Planet. Space Sci.* 46, 1583–1596, 1998.
- Ryden, K.A., Fearn, D.G., Crowther, R. Electric propulsion: a solution to end-of-life disposal of satellites? in: Flury, W. (Ed.), Proc. Second European Conference on Space Debris, ESA, Noordwijk, Netherlands, pp. 709–712, 1997..
- Soroos, M.S. The commons in the sky: the radio spectrum and geosynchronous orbit as issues in global policy. *Int. Organiz.* 36, 665–677, 1982.
- Space Track. Available at: <<http://www.space-track.org>> (accessed April 30, 2008)..
- Walker, R., Martin, C.E. Cost-effective and robust mitigation of space debris in low Earth orbit. *Adv. Space Res.* 34, 1233–1240, 2004.
- Wiedemann, C., Krag, H., Bendisch, J., Sdunnus, H. Analyzing costs of space debris mitigation methods. *Adv. Space Res.* 34, 1241–1245, 2004.